# Efficient Coding and Risky Choice*

Cary Frydman† and Lawrence J. Jin‡

July 8, 2019

## ABSTRACT

We present a model of risky choice in which the decision maker ($DM$) perceives a lottery payoff with noise due to the brain's limited capacity to represent information. We model perception using the principle of *efficient coding*, which implies that perception is most precise for frequently occurring stimuli. Our model shows that it is efficient for risk taking to be more sensitive to those payoffs that the $DM$ encounters more frequently. The model generates a value function and a probability weighting function that are similar to those in prospect theory, but it also predicts that the $DM$'s value function fluctuates with the recently encountered distribution of payoffs. To test the model, we manipulate the distribution of payoffs in a laboratory experiment. We find that risk taking is indeed more sensitive to those payoffs that are presented more frequently. We then conduct an additional experiment to test the key driving mechanism of our model, namely that the perception of a payoff is noisy and depends on the recent environment. In this second experiment, we incentivize subjects to classify which of two symbolic numbers is larger. We find that subjects exhibit higher accuracy for those numbers that they have observed more frequently. Overall, our experimental results suggest that risk taking depends systematically on the payoff distribution to which the $DM$'s perceptual system has recently adapted.

*JEL classification:* G02, G41
*Keywords:* efficient coding, perception, risky choice, neuroeconomics

*We thank Nicholas Barberis, John O'Doherty, Nicola Gennaioli, Shimon Kogan, Alex Imas, Stavros Panageas, Antonio Rangel, Andrei Shleifer, Elke Weber, Michael Woodford, Lingxuan Wu, and seminar participants at Caltech, the Chinese University of Hong Kong, the National University of Singapore, Tsinghua University, the University of Hong Kong, the University of New South Wales, the University of Technology Sydney, the University of Utah, the University of California, San Diego, the University of Southern California, Washington University in St. Louis, Yale University, the Behavioral Economics Annual Meeting, the Chicago Booth Conference in Behavioral Finance and Decision Making, the Kentucky Finance Conference, the LA Finance Day Conference, the NBER Behavioral Finance Meeting, and the Sloan-Nomis Workshop on the Cognitive Foundations of Economic Behavior for helpful comments. Frydman thanks the NSF for financial support.

†Marshall School of Business at USC. cfrydman@marshall.usc.edu, +1 (213) 821-5586.
‡Division of the Humanities and Social Sciences at Caltech. lawrence.jin@caltech.edu, +1 (626) 395-4558.

# I. Introduction

When choosing between two lotteries, the decision maker (called "*DM*" hereafter) first perceives the set of payoffs from each lottery and then executes a decision. Because there are constraints on the degree to which the brain can process information, the perception of numerical quantities is inherently noisy (Dehaene (2011)). Understanding precisely how these constraints affect perception of payoffs has the potential to generate new insights about risk taking, and in particular, its instability over time. As shown by decades of experimental studies, one source of instability is the sequence of financial outcomes that the subject has experienced: past gains and losses have a systematic effect on subsequent risk taking (Thaler and Johnson (1990); Weber and Camerer (1998); Imas (2016)). A different potential source of instability is the *DM*'s perception of a payoff, which can vary systematically with the payoffs that she has recently observed.

Why would the *DM*'s perception of a given payoff vary across different environments? If the mechanism used for perceiving payoffs is similar to the one used for perceiving sensory stimuli such as light or sound, then it may in fact be optimal to hold different perceptions of the same payoff across different environments. Specifically, a core principle in neuroscience, called *efficient coding*, states that the brain should allocate resources so that perception is relatively more precise for those stimuli that are expected to occur relatively more frequently (Barlow (1961); Laughlin (1981)). This principle explains the temporary "blindness" that we experience when moving from a dark room to a brightly lit one, because resources have not yet been adjusted for precisely perceiving objects in the new bright environment. If the principle of efficient coding extends to the domain of risky choice, it can provide a normative foundation for the variation in risk taking across environments.

In this paper, we present a model of choice under risk in which the perception of payoffs is governed by efficient coding. We then test the model experimentally by assessing how risk taking varies with the recently encountered payoff distribution. Our model builds on the theoretical work of Woodford (2012a) and Khaw, Li, and Woodford (2019) (hereafter "KLW"), who assume that the perception of payoffs is imperfect and is estimated through Bayesian inference. Specifically, KLW propose that the *DM*'s perceptual system generates a noisy signal about the true payoff value, which is then combined with her prior belief to form an estimate of the true payoff. We depart from KLW by taking the *DM*'s prior belief as a primitive, and then deriving a set of

likelihood functions through efficient coding (Wei and Stocker (2015)). These likelihood functions efficiently use limited perceptual resources, and when combined with the $DM$'s prior belief, generate a subjective value function that exhibits several features of prospect theory, including reference dependence and diminishing sensitivity (Kahneman and Tversky (1979)).[1]

Importantly, our model makes precise predictions about how these features of the value function vary with the payoff distribution to which the $DM$ has adapted. One such prediction is that Weber's law of diminishing sensitivity arises endogenously in the model when the $DM$ has adapted to a payoff distribution where smaller payoffs are more frequent than larger payoffs. More generally, we show that the degree of diminishing sensitivity over a given range of payoffs is tied directly to how frequently these payoffs occur in the recent environment. To see this, consider an environment where the upside of a risky lottery is often in the range between \$10 and \$20, in which case, efficient coding implies that perceptual resources are allocated toward discriminating between payoffs in this range. In the same environment, if the upside is occasionally increased from \$30 to \$40, then risk taking will not increase much because the $DM$'s value coding is relatively imprecise for values in this range, and thus cannot easily distinguish between these two infrequent values. However, if the overall distribution of payoffs changes, so that the upside frequently falls between \$30 and \$40, then the $DM$ can easily perceive this difference, and risk taking will increase substantially when the upside is increased from \$30 to \$40. Diminishing sensitivity therefore arises from efficient coding, and crucially, the curvature of the value function fluctuates with the payoff distribution to which the $DM$ has recently adapted.

While efficient coding generates a value function that is relatively flat over payoffs that occur infrequently, the value function exhibits its steepest slope around the most frequently occurring payoff. In particular, if we take the "reference point" in prospect theory as the value for which the $DM$ has the highest marginal utility, then efficient coding delivers the most frequently occurring payoff as the reference point. More generally, efficient coding implies that marginal utility is highest for those payoffs that occur most frequently, because these are the payoffs that the $DM$ evaluates most often. This generates a strong testable prediction, namely, that risk taking should become more sensitive to a given range of payoffs, when shifting to an environment where these payoffs

[1] When applied to probabilities, efficient coding can also generate an inverse $S$-shaped probability weighting function that is featured in prospect theory. We discuss this further in Section VI.3.

occur more frequently.

To test this prediction, we conduct a laboratory experiment in which subjects make a series of 480 decisions between a risky lottery and a certain option. While such a large number of trials is not typical in economic experiments on risky choice, this feature of our design enables us to carefully vary the payoff distribution over time within each subject. We manipulate the distribution of risky payoffs across two experimental conditions: one in which payoffs in the choice set are drawn from a distribution with high volatility, and the other in which the distribution has low volatility. All payoff values in a given block (i.e., a consecutive set of trials) are drawn from either the high volatility distribution or the low volatility distribution. Consistent with our model, we find that risk taking is more sensitive to payoffs in the low volatility blocks, compared to the high volatility blocks.[2]

We then conduct an additional experiment to further test the key mechanism of efficient coding of lottery payoffs. In this second experiment, subjects still need to perceive numerical quantities, but they do not need to perceive any probabilities or integrate them with payoffs. Instead, subjects simply classify whether a number displayed on each trial is above or below a reference number. We find that even in this simpler environment, classification accuracy depends on the distribution of numbers to which the subject has adapted. Consistent with our theory, subjects exhibit greater accuracy if the number has occurred more frequently in the recent past.

While we formally present the full model later in the paper, we briefly explain the two basic assumptions here. First, we assume that the $DM$ encodes each risky payoff with noise, where the noise structure is endogenously generated through efficient coding. Specifically, when the $DM$ is presented with a choice set in which a risky lottery pays $X$ dollars with a positive probability of $p$, we assume that the $DM$ draws a noisy signal, $R_x$, from $f(R_x|X)$—the likelihood function—which is derived from efficient coding. Second, following KLW and the literature on sensory perception, we assume that the $DM$ uses Bayesian inference to compute the optimal estimates of the numerical payoffs under consideration.[3] Importantly, in our model, both ingredients of Bayesian inference—

[2]While fatigue may affect the average level of noise in perception as the experiment progresses, our block design implies that fatigue should have a similar effect in both experimental conditions, and thus it should not impact our tests that compare these conditions. Indeed, we find that our main experimental result is robust to conditioning on the first half (or the second half) of the 480 trials.

[3]There are several studies that find a strong connection between quantitative predictions from a Bayesian framework and data from controlled experiments on sensory perception. See, for example, Stocker and Simoncelli (2006), Girshick, Landy, and Simoncelli (2011), and Wei and Stocker (2015, 2017).

the prior belief and the likelihood functions—are determined by the recent payoff distribution. Compared to earlier models that exogenously assume the likelihood functions, our model provides an extra layer of discipline in the Bayesian framework by deriving the likelihood functions through the combination of the payoff distribution and efficient coding (Wei and Stocker (2015)). In the final step of the decision making process, the $DM$ chooses the lottery with the maximum *estimated* expected value.

For most of the paper, we rely on the comparative static predictions from the model to explain our experimental data. In Section V, we present a dynamic extension of the model that explicitly incorporates the adaptation process. In this dynamic extension, we make two important assumptions that constrain the process through which the $DM$ constructs her prior. First, we assume the $DM$ updates her prior belief based on a sequence of past *perceived* payoffs. This constraint is motivated by our basic model assumption that the $DM$ cannot directly observe the true payoffs, and thus can learn only from the perceived payoffs. Second, we incorporate a well-known pattern from the memory literature by assuming that, when constructing her prior belief, the $DM$ assigns more weight to recent payoffs, compared to those in the more distant past (Kahana (2012) and Bordalo, Gennaioli, and Shleifer (2019)). We simulate the dynamic model and show that, for the set of parameters that subjects face in our experiment, the main model prediction continues to hold when the prior is given by a recency-weighted distribution of perceived payoffs.

The dynamic extension also provides a framework to better understand the interaction between memory and efficient coding. Because the $DM$ builds her prior belief based on memories of past payoffs, memory indirectly affects the likelihood functions through efficient coding. Thus, memory plays a crucial role in shaping both the prior and the likelihood functions. At the same time, efficient coding constrains the memory system, in the sense that memory only has access to past perceived payoffs, rather than past true payoffs.

At a basic level, our model is meant to capture intuitive judgments about choice under risk, such as the judgments between simple gambles that Kahneman and Tversky (1979) sought to explain with prospect theory. Our model does not apply to all decisions under risk, and in particular, it should not be applied to decisions that are based on explicit symbolic calculations. These decisions are instead likely to be governed by a distinct decision-making system (Dehaene (1992)). At the same time, our model is not necessarily confined to low-stakes decisions. We believe that it is

reasonable to apply our model in situations similar to those where prospect theory has found success (see Barberis (2013) for a review).

Our paper is related to several literatures. First, it contributes to a nascent literature that examines the effect of imperfect perception on economic choice. Woodford (2012b) and KLW provide a framework in which a $DM$ with linear utility appears risk averse if larger payoffs are encoded with more noise than smaller payoffs. We demonstrate that the coding functions assumed in KLW are consistent with efficient coding when the prior distribution is monotonically decreasing. Gabaix and Laibson (2017) show theoretically that a $DM$ with a discount factor of one appears impatient if payoffs delivered farther in the future are perceived with more noise. Steiner and Stewart (2016) show that Bayesian inference generates an overweighting of small probability events, as in prospect theory. Both of our experiments provide supporting evidence for the type of perceptual processes proposed in these Bayesian models of economic choice.

Second, our paper adds to a growing literature that builds cognitive and perceptual foundations for the psychological assumptions made in behavioral economics. For example, several behavioral models of financial markets have shown that prospect theory preferences help explain puzzling facts such as the high equity premium of the aggregate stock market and momentum of individual stocks (see Barberis (2018) for a review). Here, we build on the work by Woodford (2012b) and provide conditions under which the $DM$'s prior will generate both the value function and the probability weighting function from prospect theory. Our work is also related to Bhui and Gershman (2018), who demonstrate that efficient coding can provide a normative foundation for a memory-based model in cognitive science called "decision by sampling" (Stewart, Chater, and Brown (2006)).

Third, our results contribute to a literature that uses basic neural computations to constrain patterns of risky choice (Tymula and Glimcher (2017); Landry and Webb (2018)). A particularly relevant neural computation is called *normalization*, in which the brain normalizes stimulus values according to the distribution of values in the environment. Several experiments have found evidence consistent with normalization of value signals in the brain (Tobler, Fiorillo, and Schultz (2005); Padoa-Schoppa (2009); Carandini and Heeger (2012); Rangel and Clithero (2012); Louie and Glimcher (2012)).[4] More recently, Khaw, Glimcher, and Louie (2017) provide experimental

[4]In related theoretical work, Bushong, Rabin, and Schwartzstein (2017) develop a model based on the assumption that the $DM$'s perception of a given absolute difference depends on the range of stimulus values under consideration. Their key assumption can be motivated, in part, by the above experimental evidence on normalization.

evidence demonstrating that models of normalization can explain context-dependent valuation of consumer goods. To the extent that normalization can implement a neural code that efficiently represents value information, our experimental results are consistent with the idea that normalization may also be important in the valuation of risky lotteries (Soltani, De Martino, and Camerer (2012)).

The paper proceeds as follows. In Section II, we lay out the basic elements of the model and analyze the model's implications. Sections III and IV test the model in a risky choice experiment and a perceptual experiment, respectively. Section V develops a dynamic extension of the model. Section VI provides additional discussions. Section VII concludes and suggests directions for future research.

# II. The Model

In this section we build on the work of KLW and Wei and Stocker (2015, 2017) to develop a static model of risky choice in which the perception of payoffs is governed by efficient coding. We then use the perceived payoffs to derive the $DM$'s value function. We show precisely how variation in the $DM$'s prior belief about payoffs drives variation in the value function. In Section V, we extend the model by incorporating an adaptation process that generates predictions about the dynamics of choice.

## *1. Choice environment*

The $DM$ faces a choice set that contains two options: a certain option and a risky lottery. The certain option, denoted as $(C, 1)$, pays $C$ dollars with certainty. The risky lottery, denoted as $(X, p; 0, 1-p)$, pays $X$ dollars with a probability of $p$ and zero dollars with the remaining probability of $1 - p$. The $DM$'s task is to choose between these two options.

Under expected utility theory, a $DM$ with utility $U(\cdot)$ chooses the risky lottery over the certain option if and only if

$$p \cdot U(X) + (1 - p) \cdot U(0) \geq U(C). \tag{1}$$

Conditional on $X$, $C$, and $p$, the $DM$'s choice is non-stochastic.

Motivated by the literature on sensory perception, we depart from the expected utility framework by assuming that the $DM$ imperfectly perceives the payoffs $X$ and $C$ (Dehaene (2011); Girshick et al. (2011); Wei and Stocker (2015)).[5] We model this imperfect perception in a Bayesian framework. Specifically, we assume that before observing the choice set, the $DM$ has prior beliefs about $X$ and $C$. Upon observing the choice set, the presentations of $X$ and $C$ generate a noisy signal, $R_x$, of $X$, and a noisy signal, $R_c$, of $C$. $R_x$ is randomly drawn from a conditional distribution given $X$, denoted as $f(R_x|X)$, and $R_c$ is randomly drawn from a conditional distribution given $C$, denoted as $f(R_c|C)$. These conditional distributions are also called the likelihood functions, and they are derived through an efficient coding criterion that we specify below.

Given the prior beliefs and the likelihood functions, the $DM$ then follows Bayes' rule to form optimal estimates $\mathbb{E}[\tilde{X}|R_x]$ and $\mathbb{E}[\tilde{C}|R_c]$ where $\tilde{X}$ and $\tilde{C}$ are random variables whose distributions are the $DM$'s posterior beliefs about $X$ and $C$, respectively. These estimates are optimal in the sense that they miminize the mean squared error between the estimates and the true values of $X$ and $C$. As in KLW, we assume that the $DM$ has linear utility.[6] Therefore, the $DM$ chooses the risky lottery if and only if $p \cdot \mathbb{E}[\tilde{X}|R_x] > \mathbb{E}[\tilde{C}|R_c]$.[7]

It is worth noting that the encoding process described above—the process that maps $X$ and $C$ to $R_x$ and $R_c$—is conditional on the values of $X$ and $C$, which we assume are perfectly observable to the econometrician but not to the $DM$. That is, even after the $DM$ is presented with a choice set, she still faces uncertainty about the payoff values of $X$ and $C$. Therefore, Bayesian inference takes place at the level of a single choice set, and characterizes how the $DM$'s prior belief shifts after observing a noisy signal of the true payoff. The noisy encoding of payoffs drives our main model predictions, and in the next section, we derive the encoding process under efficient coding.

[5] Further evidence for this assumption comes from recent experimental work which demonstrates that single neurons in the human brain selectively and stochastically respond to a given number (Kutter, Bostroem, Elger, Mormann, and Nieder (2018)). Such "number neurons" are likely to generate the noisy perception of symbolic numbers.

[6] This assumption allows us to focus on how imperfect perception—rather than intrinsic risk preferences—affects risk taking.

[7] We assume for simplicity that $(i)$ the probability $p$ is perceived without noise, and $(ii)$ the probability $p$ is integrated with $\mathbb{E}[\tilde{X}|R_x]$ without noise. In Section IV, we conduct an additional experiment that provides a sharp test of the efficient coding hypothesis without appealing to these two assumptions. In Section VI.3, we further discuss our model's implications for the imperfect perception of probability.

*2. Likelihood function*

Before analyzing the encoding of the specific payoffs in our choice environment, we first consider a general stimulus value $\theta$, and its noisy signal $m$. The likelihood function $f(m|\theta)$ is the conditional probability distribution of $m$ given $\theta$. We can interpret this likelihood function as the *code* that the $DM$ uses to represent the information about $\theta$. The basic premise of efficient coding is that the $DM$ treats this code as a decision variable, and chooses one that efficiently represents the information about $\theta$.

Specifically, we follow Wei and Stocker (2015) and assume that the $DM$ chooses the likelihood function to maximize the mutual information between $\theta$ and $m$

$$\max_{f(m|\theta)} I(\theta, m) \tag{2}$$

subject to a capacity constraint

$$S \equiv \int_{\theta} \sqrt{J(\theta)} d\theta \leq C, \tag{3}$$

where $J(\theta)$ is the Fisher information of $\theta$, and it is given by

$$J(\theta) = \int \left( \frac{\partial \ell \mathrm{n} f(m|\theta)}{\partial \theta} \right)^2 f(m|\theta) dm. \tag{4}$$

Under the conditions that $f(m|\theta)$ is a normal probability density function with respect to $m$ and that the variance of this probability density function is small, Wei and Stocker (2016) show that the mutual information $I(\theta, m)$ can be approximated by

$$\frac{1}{2} \ell \mathrm{n} \left( \frac{S^2}{2\pi e} \right) - KL \left( f(\theta) || \frac{\sqrt{J(\theta)}}{S} \right), \tag{5}$$

where $KL(\cdot||\cdot)$ represents the Kullback-Leibler divergence, and $f(\theta)$ is the $DM$'s prior belief about the distribution of $\theta$. Maximizing (5) subject to the capacity constraint in (3) means that the Kullback-Leibler divergence must be zero. This requires

$$\sqrt{J(\theta)} \propto f(\theta). \tag{6}$$

In other words, the square root of Fisher information, which can be constructed from (4) using the

likelihood function $f(m|\theta)$, must be proportional to the $DM$'s prior belief $f(\theta)$.

Intuitively, the Fisher information $J(\theta)$ measures the amount of coding resources allocated toward perception of a given stimulus value $\theta$. As a result, the efficient coding condition in (6) implies that encoding accuracy is greater for stimulus values that occur more frequently.

For the rest of the paper, we use the condition in (6) to construct the likelihood function. We note that this condition is one of several potential definitions of efficient coding in the domain of risky choice. We choose this particular one because of its accuracy in modeling data from perceptual experiments (Wei and Stocker (2015)), and more recently, from an economic experiment (Polania, Woodford, and Ruff (2019)). In Section VI.1 and Appendix C, we discuss and test an alternative coding scheme that could be applied to risky payoffs.

Proposition 1 constructs a class of likelihood functions that satisfies the efficient coding condition in (6).

**Proposition 1.** *Assume the $DM$'s prior belief about the distribution of $\theta$ is $f(\theta)$, where $\theta$ takes the range of $(-\infty, \infty)$. The cumulative density function of this distribution is $F(\theta) = \int_{-\infty}^{\theta} f(\xi)d\xi$. Then for each $\theta$, the following likelihood function*

$$f(m|\theta) = \frac{1}{\sqrt{2\pi}\cdot\sigma}\exp\left(-\frac{(F(\theta)-m)^2}{2\sigma^2}\right) \tag{7}$$

*satisfies the efficient coding condition in (6), where $m$ also takes the range of $(-\infty, \infty)$.*

*Proof.* See Appendix A.1. ■

The likelihood function in (7) contains one free parameter, $\sigma$, which represents the amount of internal noise in the $DM$'s perceptual system. If the $DM$ is endowed with a small amount of coding resources, then $\sigma$ will be large, and thus the likelihood function will be noisy. Conversely, as the amount of coding resources tends to infinity, $\sigma$ converges to zero; in this case, the $DM$ encodes all payoffs without noise and our model reduces to expected utility theory.

In order to illustrate the implications of Proposition 1 for risky choice, we first specify the stimulus value $\theta$ to be $X$ or $C$, and specify the associated noisy signal $m$ to be $R_x$ or $R_c$. We then

assume that the true stimulus distributions of $X$ and $C$ are lognormal:

$$\begin{aligned} f(X;\mu_x,\sigma_x) &= \frac{1}{\sqrt{2\pi}\cdot\sigma_x X}\exp\left(-\frac{(\ell\text{n}X-\mu_x)^2}{2\sigma_x^2}\right), \\ f(C;\mu_c,\sigma_c) &= \frac{1}{\sqrt{2\pi}\cdot\sigma_c C}\exp\left(-\frac{(\ell\text{n}C-\mu_c)^2}{2\sigma_c^2}\right). \end{aligned} \tag{8}$$

We will use this same type of lognormal stimulus distributions later in the laboratory experiment. Finally, we assume that the $DM$'s priors about the distributions of $X$ and $C$ coincide with the true stimulus distributions[8]

$$f_0(X) = f(X;\mu_x,\sigma_x), \qquad f_0(C) = f(C;\mu_c,\sigma_c). \tag{9}$$

Given the assumptions of (8) and (9), the likelihood functions of $X$ and $C$ are:

$$\begin{aligned} f(R_x|X) &= \frac{1}{\sqrt{2\pi}\cdot\sigma}\exp\left(-\frac{(\Phi((\ell\text{n}X-\mu_x)/\sigma_x)-R_x)^2}{2\sigma^2}\right), \\ f(R_c|C) &= \frac{1}{\sqrt{2\pi}\cdot\sigma}\exp\left(-\frac{(\Phi((\ell\text{n}C-\mu_c)/\sigma_c)-R_c)^2}{2\sigma^2}\right). \end{aligned} \tag{10}$$

The expressions in (10) show that the presence of internal noise ($\sigma > 0$) makes these likelihood functions depend directly on the parameters of the stimulus distributions, $\mu_x$, $\sigma_x$, $\mu_c$, and $\sigma_c$.[9] As a result, the variation in the stimulus distribution becomes a key source of variation in the perception of payoffs.

To illustrate the dependence of perception on the stimulus distribution, Figure 1 plots the lognormal stimulus distribution of $X$ specified in (8) with two different levels of volatility: in the low volatility case, we set $\sigma_x$ to 0.19; and in the high volatility case, we set $\sigma_x$ to 0.55. Figure 1 also plots, for each volatility level, a set of implied likelihood functions. Here, we treat the likelihood function $f(R_x|X)$ as a function of $X$ for each value of $R_x$. We plot the likelihood function for several values of $R_x$: 0.15, 0.2, 0.5, 0.8, and 0.85. To get a sense of these values of $R_x$, we compute

[8]This assumption can be justified if the $DM$ has fully adapted to the stimulus distribution, and thus is meant to capture beliefs in a "steady state." In Section V, we relax the assumptions in (9) and develop an extension of the model in which we explicitly incorporate the adaptation process.

[9]As $\sigma$ converges to zero, the relation between the signal ($R_x$ or $R_c$) and the stimulus value ($X$ or $C$) becomes a deterministic one-to-one mapping. In this limiting case, the parameter values of $\mu_x$, $\sigma_x$, $\mu_c$, and $\sigma_c$ do not affect the perception of $X$ or $C$.

the unconditional distribution of $R_x$ as

$$f(R_x) = \int_0^\infty f(R_x|X)f(X)dX. \tag{11}$$

We find that large values of $X$—values from the right tail of the lognormal distribution $f(X; \mu_x, \sigma_x)$—tend to generate values of $R_x$ that are close to one (for example, $R_x = 0.85$ or $0.8$). Conversely, small values of $X$ tend to generate values of $R_x$ that are close to zero (for example, $R_x = 0.15$ or $0.2$).[10]

**[Place Figure 1 about here]**

Figure 1 highlights some important features of the likelihood function $f(R_x|X)$. First, for a given stimulus distribution, the shape of the likelihood function depends significantly on the value of $R_x$. Consistent with the core principle of efficient coding, those values of $X$ that occur frequently tend to generate moderate values of $R_x$ which give rise to likelihood functions with low dispersion. Conversely, those values of $X$ that occur infrequently tend to generate extreme values of $R_x$ which give rise to likelihood functions with high dispersion. Second, for each value of $R_x$, changing the stimulus distribution—in particular, changing $\sigma_x$—alters the shape of the likelihood function. A stimulus distribution with lower volatility will generate a likelihood function with lower dispersion. Intuitively, when the stimulus distribution has lower volatility, the $DM$ allocates her finite coding resources to a narrower range of stimulus values, resulting in higher discriminability between these stimulus values (as measured by the lower dispersion of the likelihood function).

### *3. Bayesian inference*

The $DM$ uses the likelihood function derived in the previous section, in conjunction with her prior belief about the stimulus distribution, to form a posterior distribution about each payoff in the choice set. We assume that the $DM$ uses the mean of the posterior distribution as her estimate of each payoff. Specifically, the posterior means of $X$ and $C$, conditional on $R_x$ and $R_c$, are given

[10] It is easy to check that the distribution $f(R_x)$ defined in (11) does not depend on the parameters $\mu_x$ and $\sigma_x$ in (8): all continuous stimulus distributions lead to the same $f(R_x)$. Moreover, as $\sigma$ in (10) goes to zero—that is, as the amount of coding resources tends to infinity—$f(R_x)$ converges to a uniform distribution between zero and one. In Appendix A.2, we provide a more detailed discussion of these properties of $f(R_x)$.

by

$$\mathbb{E}[\tilde{X}|R_x] \equiv \int_0^\infty f(X|R_x)XdX = \frac{\int_0^\infty f(R_x|X)f_0(X)XdX}{\int_0^\infty f(R_x|X)f_0(X)dX} \tag{12}$$

and

$$\mathbb{E}[\tilde{C}|R_c] \equiv \int_0^\infty f(C|R_c)CdC = \frac{\int_0^\infty f(R_c|C)f_0(C)CdC}{\int_0^\infty f(R_c|C)f_0(C)dC}, \tag{13}$$

where the $DM$'s prior beliefs, $f_0(X)$ and $f_0(C)$, are from (9), and the likelihood functions, $f(R_x|X)$ and $f(R_c|C)$, are from (10). Moreover, by Bayes' rule, the posterior distributions are

$$f(X|R_x) = \frac{f(R_x|X)f_0(X)}{\int_0^\infty f(R_x|X)f_0(X)dX} \tag{14}$$

and

$$f(C|R_c) = \frac{f(R_c|C)f_0(C)}{\int_0^\infty f(R_c|C)f_0(C)dC}. \tag{15}$$

After the $DM$ forms a posterior belief for each payoff, she then chooses the risky lottery if and only if $p \cdot \mathbb{E}[\tilde{X}|R_x] > \mathbb{E}[\tilde{C}|R_c]$. The left hand side of this inequality provides the $DM$'s estimated expected value of the risky lottery, while the right hand side provides her estimated expected value of the certain option.

### *4. Value function*

The noisy encoding process described above implies that the same payoff $X$ will generate different noisy signals when it is presented on different occasions. Given that each realized value of the noisy signal $R_x$ maps to a different posterior mean as shown in (12), the $DM$ faces a distribution of subjective valuations for each value of $X$. Importantly, the *average* subjective valuation of $X$, which we call the value function, will in general be different from $X$ itself.

Specifically, we define the value function, $v(X)$, by

$$v(X) = \int_{-\infty}^\infty \mathbb{E}[\tilde{X}|R_x]f(R_x|X)dR_x. \tag{16}$$

That is, $v(X)$ represents the subjective valuation of $X$ averaged over the conditional probability density $f(R_x|X)$. Given the randomness in the noisy signal $R_x$, we also compute the standard deviation for the subjective valuation of $X$:

$$\sigma(X) = \left[\int_{-\infty}^{\infty} \left(\mathbb{E}[\tilde{X}|R_x]\right)^2 f(R_x|X)dR_x - v^2(X)\right]^{1/2}. \tag{17}$$

Equations (16) and (17), together with equation (12), indicate that the curvature of the value function and the randomness in the subjective valuation are jointly determined by the $DM$'s prior belief about the payoff distribution and the implied likelihood functions. As a result, the variation in the lognormal stimulus distribution $f(X; \mu_x, \sigma_x)$ gives rise to *predictable* variation in $v(X)$ and $\sigma(X)$. To illustrate these model implications, Panel A of Figure 2 plots, for both $\sigma_x = 0.19$ (low volatility) and $\sigma_x = 0.55$ (high volatility), the average subjective valuation $v(X)$, as well as its one-standard-deviation bounds $v(X) \pm \sigma(X)$.

**[Place Figure 2 about here]**

Panel A of Figure 2 leads to several observations. First, the lack of discriminability among outliers generates diminishing sensitivity: the marginal utility $v'(X)$ decreases as $X$ becomes very large. At the same time, $v'(X)$ also decreases as $X$ becomes very small; this is because under a lognormal distribution, small positive values are also perceived as outliers.[11] Second, diminishing sensitivity is more pronounced when the volatility of the stimulus distribution is lower. In this case, the $DM$ is frequently exposed to a narrower range of stimulus values, and therefore finds it difficult to discriminate among a wider range of stimuli that she perceives as outliers. Third, the curvature in the value function is negatively related to the randomness in the subjective valuation: for very large values of $X$, low discriminability leads to both lower marginal utility $v'(X)$ and higher randomness in utility, $\sigma(X)$. Finally, the value of $X$ for which $v(X)$ attains its greatest slope, which typically corresponds to the "reference point" in prospect theory, arises endogenously in our framework. In our model, the reference point corresponds to the stimulus value that the $DM$ expects to occur with the highest frequency, and thus has the highest degree of local discriminability.

As mentioned above, the lack of discriminability among outliers in both tails of the lognormal

[11] Payzan-LeNestour and Woodford (2019) provide experimental evidence from a perceptual task that is consistent with the prediction of insensitivity to outlier values.

stimulus distribution generates diminishing sensitivity for both very small and very large payoffs. In other words, the hump shape of the lognormal distribution tends to generate an $S$-shaped value function, which is distinct from a concave value function typically assumed in prospect theory over *all* positive payoffs (Kahneman and Tversky (1979); Tversky and Kahneman (1992)). Interestingly, efficient coding can also generate this more familiar value function if the $DM$ discriminates very well between small payoffs, but has difficulty discriminating between large payoffs. What type of stimulus distribution would lead to this particular pattern of discriminability?

A monotonically decreasing stimulus distribution would produce exactly this. Specifically, when the $DM$ faces a distribution in which small payoffs are more probable than large payoffs, it is then optimal for the $DM$ to discriminate more precisely between these small numbers at the expense of discriminating precisely between large numbers.[12] In Panel B of Figure 2, we plot an example of a monotonically decreasing stimulus distribution—a gamma distribution—and the implied value function. We find that this value function is indeed concave. The comparison of the value functions in Panel A and Panel B of Figure 2 highlights an important implication of our model: the shape of the value function is *malleable* yet is tied closely to the underlying stimulus distribution.

In summary, the malleability of the value function arises from the variation in the stimulus distribution. An important feature of our model is that we can construct the value function for *any* continuous stimulus distribution. Because our laboratory experiment focuses on manipulating the volatility of the stimulus distribution, we retain the lognormality assumption of (8) for the rest of the model section.[13]

[12] When the $DM$ has a prior belief that is monotonically decreasing, the likelihood functions generated by efficient coding exhibit "scalar variability," the notion that the likelihood function becomes more dispersed as the stimulus magnitude increases. Evidence for this property is commonly found in experiments on numerical cognition (Dehaene (2011)). Moreover, when the $DM$'s prior belief is monotonically decreasing, our model of efficient coding endogenously generates likelihood functions that also resemble the logarithmic encoding functions assumed in KLW. Interestingly, there is evidence that a monotonically decreasing prior is a good approximation for the distribution of naturally occurring numbers (Dehaene and Mehler (1992)). Therefore, our model of efficient coding, when combined with the distribution of naturally occurring numbers, can be seen as providing a plausible microfoundation for the logarithmic encoding functions in KLW.

[13] One could also manipulate the volatility of a stimulus distribution that is monotonically decreasing. However, such a manipulation would also strongly affect the mean and skewness of the distribution, which can lead to confounds in testing the effect of efficient coding on choice behavior.

### 5. *Probability of risk taking*

As we described in the previous section, efficient coding implies that marginal utility is high for those payoffs that occur frequently, because these are the payoffs that the $DM$ can precisely discriminate between. This model implication generates a strong testable prediction: risk taking should be more sensitive to a given range of payoffs when shifting to an environment where these payoffs occur more frequently. To examine this prediction, we first compute the probability of risk taking, that is, the probability of choosing the risky lottery over the certain option. To do so, recall that, conditional on $X$ and $C$, the noisy signals $R_x$ and $R_c$ are drawn from the probability density functions $f(R_x|X)$ and $f(R_c|C)$. For a given realization of $(R_x, R_c)$, the $DM$ then chooses between the risky lottery and the certain option based on the posterior means of $X$ and $C$ in equations (12) and (13). As a result, when holding $X$, $C$, and the stimulus distributions fixed, we can compute the probability of risk taking over many realizations of $R_x$ and $R_c$,

$$\mathbb{P}\text{rob}(\textit{risk taking}|X, C) = \int_{-\infty}^{\infty}\int_{-\infty}^{\infty} \mathbb{1}_{\{p\cdot\mathbb{E}[\tilde{X}|R_x]>\mathbb{E}[\tilde{C}|R_c]\}} f(R_x|X)f(R_c|C)dR_x dR_c. \tag{18}$$

To understand the determinants of the probability of risk taking, Figure 3 plots this probability against the natural logarithm of $X$ over $C$, $\ell\text{n}(X/C)$, for different volatility levels of the stimulus distributions: $\sigma_x = \sigma_c = 0.4$, 0.8, and 1.5. Specifically, for each volatility level, we set $C$ to its mean value, $\exp(\mu_c + \frac{1}{2}\sigma_c^2)$, and vary the value of $X$.

**[Place Figure 3 about here]**

Naturally, a higher ratio of $X$ over $C$ increases the attractiveness of the risky lottery and hence increases the probability of risk taking. Notice that, under expected utility theory and with no background wealth, the probability of risk taking should be a step function of $\ell\text{n}(X/C)$ with a single step at $\ell\text{n}(X/C) = \ell\text{n}[U^{-1}((U(C) - (1-p)U(0))/p)/C]$. However, in our model, the probability of risk taking has an $S$-shaped relationship with $\ell\text{n}(X/C)$. Furthermore, the overall slope of this function is *negatively* related to the volatility of the stimulus distribution. That is, risk taking is more sensitive to payoff values that are drawn from the low volatility condition. Intuitively, lower stimulus volatility reduces the range of the stimulus values that subjects are adapted to, and hence increases the encoding accuracy and the discriminability among the stimulus values within this

narrower range.[14] This is the main prediction that we test below in our experiments.

# III. An Experimental Test

In this section, we provide an experimental test of our model. Our experiment is designed specifically to test whether risk taking varies with the payoff distribution that subjects encounter.

## *1. Design*

On each trial in the experiment, subjects choose between a risky lottery and a certain option. The risky lottery delivers a positive payoff $X$ with a positive probability of $p$, and zero otherwise. The certain option delivers a positive payoff $C$ with certainty. The experiment consists of eight blocks, with sixty trials in each block. Each subject therefore completes a total of four hundred eighty trials, which we index by $t = 1, 2, \ldots, 480$. At the end of the experiment, subjects are paid according to their decision on one randomly selected trial.

We experimentally manipulated the distribution from which payoffs in the choice set are drawn. On each trial, the values of $X$ and $C$ were jointly drawn from a lognormal distribution,

$$\begin{pmatrix} \ell \mathrm{n} X \\ \ell \mathrm{n} C \end{pmatrix} \sim \mathcal{N}\left( \begin{pmatrix} \mu_x \\ \mu_c \end{pmatrix}, \begin{pmatrix} \sigma_x^2 & \rho\sigma_x\sigma_c \\ \rho\sigma_x\sigma_c & \sigma_c^2 \end{pmatrix} \right). \tag{19}$$

We set the mean values, $\mu_x$ and $\mu_c$, to 3.05 and 2.35, respectively, so that on average, the risky lottery offers a higher expected value than the certain option. Our treatment variable is the standard deviation, which we varied across two conditions: high volatility and low volatility. In the high volatility condition, we set $\sigma_x = \sigma_c = 0.55$, and in the low volatility condition, we set $\sigma_x = \sigma_c = 0.19$. The first block of the experiment was a high volatility block, and the blocks alternated deterministically, ending with a low volatility block; our experimental design is illustrated

[14] More generally, equation (18) implies that the probability of risk taking is a two-dimensional function of $X$ and $C$. In Appendix B, Figure B1 plots this probability for two different volatility levels of the stimulus distribution: $\sigma_x = \sigma_c = 0.19$ (low volatility) and $\sigma_x = \sigma_c = 0.55$ (high volatility). Figure B1 makes it obvious that $\ell\mathrm{n}(X/C)$ is not a sufficient statistic of the probability of risk taking; instead, $X$ and $C$ jointly affect this probability. For instance, with $\sigma_x = \sigma_c = 0.55$, $\mu_x = 3.05$, and $\mu_c = 2.35$, setting $X$ to 24.6 and setting $C$ to 12.2 give $X/C = 2.01$ and a risk taking probability of 77.7%. On the other hand, setting $X$ to 38.7 and setting $C$ to 19.2 give the same ratio of $X/C = 2.01$ but a lower risk taking probability of 74.3%. Therefore, our model predicts that risk taking is not "scale invariant," a point which we analyze in further detail in Appendix B.

in Figure 4. We set the correlation between $\ell n(X)$ and $\ell n(C)$ at $\rho = 0.5$. Although this positive correlation is not part of the model we developed in the previous section, it helped to reduce the number of trivial choice sets where $X < C$ (and as a result, the certain option stochastically dominates the risky lottery). The values of $X$ and $C$ were drawn from their associated distribution (high volatility or low volatility) at the subject-trial level, and thus each subject faced a unique path of payoffs during the experiment.

**[Place Figure 4 about here]**

For all trials, we set the probability that the risky lottery paid $X$ to $p = 0.59$. Following KLW, we chose this design feature for two reasons. First, we used a "non-round" number so that subjects could not easily compute the expected value of the risky lottery—such an easy computation was more likely if we used, for example, $p = 0.5$ or $p = 0.6$. Second, even though our model assumes that the subject does not encode the probability $p$ with noise, in reality, the encoding of probability can be noisy. As such, presenting the same value of 0.59 on each trial increased the plausibility of our simplifying assumption that subjects precisely encoded this particular probability value. In Section IV, we conduct an additional experiment to directly test the noisy encoding of payoffs, without appealing to any assumptions about probability encoding.

Before the experiment began, subjects were told that they would be asked to choose between two lotteries on each of four hundred eighty trials and these trials would be separated into eight parts. However, subjects were not given any information about the distributions of $X$ and $C$, nor were they told that these distributions changed across blocks. We chose not to provide subjects with this information because it allowed us to study the implications of efficient coding without imposing any specific structure on the subject's prior beliefs at the beginning of the experiment. The exact instructions that were given to subjects before the experiment are provided in Appendix E.

### *2. Experimental procedures*

We recruited $N = 34$ subjects for this experiment, which was conducted across three sessions at Caltech and USC. Before starting the experiment, subjects went through a set of ten practice trials to become familiar with the task and the software. Figure 4 provides an example trial from the experiment, in which the risky lottery is presented on the left as a colored bar chart, and the

value $X$ is displayed at the bottom next to its associated probability of 0.59. The certain option is presented on the right side of the screen. On each trial, subjects were instructed to select the left or right option by pressing one of two keys. The location of the risky lottery was randomized across subjects and trials, and subjects had unlimited time to make their decision on each trial. At the end of each block of sixty trials, a progress screen appeared, which reported how many of the eight blocks the subject had completed.

At the end of the eighth block, the computer randomly selected one of the four hundred eighty trials from the experiment. If the subject chose the risky lottery on this trial, a random number generator determined whether the subject received the payoff of $\$X$ or the payoff of \$0, according to the probabilities associated with these payoffs. If the subject chose the certain option, she received the amount of $\$C$. In addition to the earnings from this randomly selected trial, each subject received a \$7 show-up fee. The average earning, including the show-up fee, was \$25.89.

## *3. Experimental results*

### 3.1. Treatment effects

Subjects chose the risky lottery on 40.5% of trials in the low volatility condition and on 42.7% of trials in the high volatility condition. One subject did not exhibit any variation in risk taking in the low volatility condition (choosing the certain option on each trial), and we exclude this subject from all subsequent analyses.

**[Place Figure 5 about here]**

Figure 5 plots the proportion of trials on which subjects chose the risky lottery, as a function of the natural logarithm of $X$ over $C$, $\ell\text{n}(X/C)$. Recall that the probability $p$ stays constant across all trials, and therefore $\ell\text{n}(X/C)$ provides a good—though insufficient—statistic that summarizes the attractiveness of the risky lottery relative to the certain option. The figure shows that risk taking increases in $\ell\text{n}(X/C)$ in both volatility conditions; this provides a basic consistency check on the data. One can also see that the slope of the curve in the low volatility condition appears to be steeper than that in the high volatility condition. This is consistent with a basic prediction of our model: when the stimulus distribution becomes more concentrated, choice sensitivity increases.

To conduct formal empirical tests, we run regressions where the dependent variable takes the value of one (zero) if the subject chose the risky lottery (certain option) on trial $t$. We pool all 15,840 trials across subjects and conditions, and run the following logistic regression:

$$\text{risky}_t = \alpha + \beta_1 \cdot high_t + \beta_2 \cdot \ell\text{n}(X_t/C_t) + \beta_3 \cdot \ell\text{n}(X_t/C_t) \times high_t + \varepsilon_t, \tag{20}$$

where $high_t$ is a dummy variable that takes the value of one if trial $t$ is in the high volatility condition, and zero otherwise.[15] In Column (1) of Panel A of Table 1, the estimated coefficient on $\ell\text{n}(X/C)$ is significantly positive, indicating that the probability of risk taking in the low volatility condition increases in $\ell\text{n}(X/C)$. The coefficient on the interaction term $\ell\text{n}(X/C) \times high$—which is the coefficient of interest—is significantly negative, indicating that risk taking becomes less sensitive to $\ell\text{n}(X/C)$ in the high volatility condition. This provides formal support for a difference in choice sensitivity between the high and low volatility conditions.

**[Place Table 1 about here]**

Our model predicts that this difference in choice sensitivity stems from different *perceptions* of $X$ and $C$ across conditions. However, the distributions of $X$ and $C$ themselves vary across conditions, and thus the difference we detect may simply be driven by a different response to extreme values of $\ell\text{n}(X/C)$. In particular, the range of $\ell\text{n}(X/C)$ in the low volatility condition is (0.02, 1.36). However, in the high volatility condition, there are many trials for which $\ell\text{n}(X/C)$ falls outside this range.

To help address this concern, we restrict our regression to trials with similar levels of $\ell\text{n}(X/C)$ across the two volatility conditions. We re-estimate the regression in Column (1) using only trials for which $0.02 < \ell\text{n}(X/C) < 1.36$; this represents the set of values of $\ell\text{n}(X/C)$ which appear in *both* conditions of our experiment. Column (2) shows that our results are quite similar on this subset of data. It is therefore unlikely that differences in the current choice set drive the full effect; however, we note that this is not a perfect control because the distribution of $\ell\text{n}(X/C)$ still differs across volatility conditions, even within this restricted domain. Column (3) is estimated using data from

[15] All regression results reported in Table 1 are robust to an alternative mixed-effects logistic regression specification, in which we include a random intercept, and a random slope on both $\ell\text{n}(X/C)$ and $\ell\text{n}(X/C) \times high$. In the next section, we explicitly investigate hetereogeneity across subjects.

the first half of each block (the first thirty trials), while Column (4) uses data from the second half (the last thirty trials). We find that the main result holds in both of these subsets of the data. Finally, Column (5) shows our results hold even within the first ten trials of each block.[16]

### 3.2. Heterogeneity across subjects

**[Place Figure 6 about here]**

The data presented in Figure 5 are pooled across subjects, and therefore mask any individual heterogeneity in the change in risk taking across volatility conditions. To investigate the extent of this heterogeneity, for each subject and condition, we run the following logistic regression:

$$\text{risky}_t = \alpha + \beta \cdot \ell\text{n}(X_t/C_t) + \varepsilon_t \tag{21}$$

across all trials indexed by $t$. We record the estimates of $\beta$ for each subject in the high and low volatility conditions, and plot these estimates against each other in Figure 6. We observe substantial heterogeneity across subjects in the sensitivity of risk taking with respect to $\ell\text{n}(X/C)$. Furthermore, those subjects who are most sensitive to payoffs in the high volatility condition are also most sensitive to payoffs in the low volatility condition. This result indicates that within subjects, the parameter $\sigma$—which measures the internal noise in the subject's perceptual system—is relatively stable across volatility conditions. Most importantly, we find that for a majority of subjects, the data lie above the forty-five degree line. This result implies that the treatment effect we found at the group level is also present at the individual level for most of our subjects.

### 3.3. Assumptions about noiseless encoding process

All the implications of our model are driven by the noisy encoding of $X$ and $C$. In particular, we make two simplifying assumptions: $(i)$ there is no noise in encoding the probability $p$, and $(ii)$ there is no noise in computing the product of $p$ and $\mathbb{E}[\tilde{X}|R_x]$. In reality, there is likely to be noise in

[16] We note that in each specification in Panel A, the coefficient on the *high* dummy variable is significantly positive. A possible reason for this result is that $\ell\text{n}(X/C)$ is not a sufficient statistic for risk taking, and therefore may contribute to model misspecification. Panel B of Table 1 presents regression results where we separately enter the $X$ and $C$ regressors, as well as their associated interaction terms. We find that the coefficient on the *high* dummy variable is no longer significant in these regressions. We also find that risk taking remains less sensitive to both $X$ and $C$ in the high volatility condition, compared to the low volatility condition.

both of these processes, which could potentially be responsible for some of the above experimental results.

To provide a sharper test of the effect of noisy encoding of payoffs, we run an additional experiment, in which the subject still needs to perceive $X$, but does not need to perceive the probability $p$ or integrate probabilities with payoffs. Given that the noisy encoding of payoffs is sufficient to generate our main theoretical predictions, we should still find evidence that the perception of $X$ depends on the recent stimulus distribution, even when there is no need to perceive the probability $p$.

# IV. An Additional Perceptual Experiment

## *1. Design*

The design of our second experiment is informed by work from the literature on perception of numerical quantities (Moyer and Landauer (1967)). Our experimental design builds on that of Dehaene, Dupoux, and Mehler (1990), who present subjects with an Arabic numeral between 31 and 99 on each trial of their experiment. The subject's task is simply to classify whether the Arabic numeral presented on the screen is larger or smaller than the reference level of 65. Their main result is that as the stimulus numeral gets closer to the reference level, response times increase and classification accuracy decreases. These results are consistent with the noisy encoding of Arabic numerals, which lies at the foundation of our model of risk taking.

One notable feature of the Dehaene et al. (1990) experiment is that the stimulus distribution is held constant throughout the experiment. Here, we exogenously vary the stimulus distribution, in much the same way that we varied the distribution of monetary amounts in our previous experiment. We have a high volatility distribution (uniform over integers in the range $[31, 99]$) and a low volatility distribution (uniform over integers in the range $[51, 79]$). Subjects are incentivized to correctly classify whether each Arabic numeral, which we denote by $X$, is larger or smaller than 65, over sixteen blocks of trials. The blocks alternate between the high volatility condition and the low volatility condition. Each block consists of eighty trials, for a total of 1,280 trials per subject. We illustrate our experimental design in Figure 7.

**[Place Figure 7 about here]**

We pay subjects based on both the accuracy and speed of their classifications. In addition to a \$7 participation fee, subjects earn a payoff of $\$(20 \times accuracy - 10 \times avgseconds)$, where *accuracy* is the percentage of correctly classified trials, and *avgseconds* is the average response time (in seconds) across all trials in the experiment. In this design, subjects still need to perceive the value $X$, but there are no probabilities to encode, nor any need to integrate probabilities with payoffs. Therefore, this design provides a clean setting in which we can test whether the perception of an Arabic numeral, $X$, depends on the recently observed stimulus distribution.

### *2. Experimental procedures*

We recruited an additional $N = 13$ subjects from Caltech for this experiment. Before the first block, subjects went through a set of ten practice trials to become familiar with the task. On each trial, the stimulus numeral was displayed in white font against a black background, on the center of the screen (Figure 7). Subjects were instructed to press one of two keys to indicate whether the stimulus was smaller or greater than 65. After responding on each trial, a white fixation cross appeared for 500 milliseconds, followed by the stimulus from the next trial. At the end of each block of eighty trials, a progress screen appeared, which reported how many of the sixteen blocks remained. The progress screen was self-paced, and subjects were given the opportunity to take a break during this screen. The average earning, including the show-up fee, was \$20.58.

### *3. Experimental results*

Subjects accurately classified the stimuli on 90.4% of trials with an average response time of 0.45 seconds. Figure 8 shows the proportion of trials that subjects classified the stimulus as greater than 65, for each value of $X$. If subjects had accurately classified all stimuli, the figure would generate a step function, with a single step at $X = 65$. Instead, the figure replicates results from several previous experiments in the literature, which show that errors decrease in the distance between the two numbers under comparison (Moyer and Landauer (1967); Dehaene et al. (1990)). To be clear, while it is unsurprising that subjects make errors in general, the more important result is that the error rate is correlated with the distance between the stimulus number and the reference level of 65.

It is also worth noting that the average subject from Caltech has very high mathematical aptitude, and thus the error rates reported here are likely to be close to a lower bound for the error rates among other samples.[17]

**[Place Figure 8 about here]**

Turning to a comparison of our two experimental conditions, we find that subjects correctly classified stimuli on 91.4% of trials in the high volatility condition, and on 89.4% of trials in the low volatility condition. A more informative statistic is the difference in accuracy between conditions, when restricting to stimuli that are common to both conditions: $51 \leq X \leq 79$. This controls for the fact that, on average, trials in the high volatility condition are "easier," in the sense that the average distance to the reference level is greater than in the low volatility condition. We find that accuracy among this subset of trials in the high volatility condition is 86.5%, which is significantly lower than the 89.4% accuracy in the low volatility condition ($p$-value = 0.004). This is consistent with the efficient coding hypothesis: in the low volatility condition, subjects adapt and devote more coding resources to the concentrated range $51 \leq X \leq 79$. In the high volatility condition, subjects need to "spread" these coding resources over a wider range, which leads to increased noise when encoding stimuli in the concentrated range (relative to the low volatility condition).

**[Place Table 2 about here]**

A sharper test of the efficient coding hypotheses is to compare the slopes in Figure 8. As in our previous experiment, we expect a steeper slope in the low volatility condition. The figure provides suggestive visual evidence for a difference in slopes. To formally test this, we run a series of logistic regressions. The dependent variable in our logistic regression takes on the value of one if the subject classified $X$ as above 65, and zero otherwise. Column (1) of Table 2 shows that the coefficient on $\ell\text{n}(X/65)$ is significantly positive, indicating that subjects' propensity to classify $X$ as greater than 65 is increasing in $\ell\text{n}(X/65)$. More importantly, we find that the coefficient on the interaction term, $\ell\text{n}(X/65) \times high$, is significantly negative, indicating that choices are noisier on trials in the high volatility condition.

[17] There is evidence that accurate perception of *non-symbolic* representations of numbers (e.g., a visual array of dots) is positively correlated with mathematical aptitude (Halberda, Mazzocco, and Feigenson (2008)), though it is unclear whether this correlation extends to tasks like ours that use symbolic numerical representations.

To control for the difference in distributions of $X$, we re-estimate the regression using data only in the range $51 \leq X \leq 79$. When restricting to this range, the distribution of $X$ is the same across both conditions, and the only difference is the distribution of previously encountered stimuli. Column (2) provides these estimation results, and we find the slope remains steeper in the low volatility condition (although the difference in slopes is smaller compared to the estimates using the full sample in Column (1)).

One assumption we make in interpreting the results in these first two columns, is that there is no "external stimulus" noise: the stimulus number is displayed clearly on the screen and the font is easy to read (as opposed to, e.g., fuzzy text). We assume that the noise that corrupts the mental representation of the stimulus is based on the internal noise in the subject's nervous system. Nonetheless, it is plausible that comparing 59 with 65 may be easier than comparing 60 with 65, not because of the distance, but because the first digits in the former comparison are more visually distinct. To address this, we re-estimated the regression in Column (1) using only trials for which the first digit differs from the first digit of the reference level: $X < 60$ or $X \geq 70$. Column (3) shows that the slope in the low volatility condition remains steeper, indicating that such a "first-digit" effect cannot explain the full extent of the shift in slope.

To summarize this experiment, we find that the accuracy of classifying an Arabic numeral is affected by $(i)$ the distance to a reference level, and $(ii)$ the distribution of previously encountered stimuli. The latter result provides useful evidence supporting a basic assumption of our model of risky choice. Specifically, in a classification task where there is no need to encode probabilities or integrate with payoffs, we find that choice sensitivity depends on the distribution of previously encountered stimuli.

## V. Dynamic Extension of the Model

In order to interpret our experimental results using the static model developed in Section II, we assumed that the $DM$'s prior beliefs coincide with the true payoff distributions (equation (9)). This assumption implies that subjects fully and instantaneously adjust their prior beliefs about the payoff distributions at the beginning of each block. In reality, however, adaptation to the statistics of the current environment occurs gradually over time. Moreover, with noisy perception, subjects

cannot directly observe the true payoff values on each trial. Therefore, the input to the adaptation process can only be based on the noisy signals—as well as the implied estimates—of the true payoff values (Robson and Whitehead (2018)).

In this section, we lay out a model of adaptation in which the $DM$ uses a sequence of past *perceived* payoffs to form her prior belief about the current payoff distribution. This dynamic model allows us to assess whether our main model prediction—that risk taking is more sensitive to payoff values in the low volatility condition—also follows when the $DM$'s prior beliefs are constructed from a sequence of past, and imperfectly perceived, payoffs.

The adaptation process we present below is motivated by recent evidence suggesting that adaptation is based on at least two components. First, there is a slow-moving component that reflects the $DM$'s long-term experience outside of the current context. Second, there is a more rapid component which adapts quickly based on local context that changes over the course of an experimental session (Burke, Baddeley, Tobler, and Schultz (2016); Zimmermann, Glimcher, and Louie (2018); Conen and Padoa-Schioppa (2019)). We note that incorporating a slow-moving component into the adaptation process can be disadvantageous because it prevents the $DM$ from completely adapting to the current local context. However, as we explain later, this component also enables the $DM$ to flexibly respond to changes in the environment, because the slow-moving component helps maintain some perceptual resources for unexpected stimuli that arrive when the local context changes.

### *1. Model setup*

We consider an environment with $T$ dates, $t = 1, \ldots, T$; $t = 1$ can be viewed as the beginning of the experiment. At each date $t$, the $DM$'s prior belief about the distribution of $X$ contains two components. The first, stable component, denoted as $l(X)$, represents the belief the $DM$ formed *before* participating in the experiment; this component does not vary with time $t$. The second, fasting-moving component is a weighted average of past perceived values of $X$ starting from $t = 1$, $\{\mathbb{E}_{t-i}[\tilde{X}_{t-i}|R_{x,t-i}]\}_{i=1}^{t-1}$; this fast-moving component allows past perceived payoffs to directly drive changes in the $DM$'s belief throughout the experiment.

Specifically, we assume that at time $t$, before observing $X_t$, the $DM$'s prior belief about the

distribution of $X$ is

$$f(X;\lambda) = \left\{ \begin{array}{c} (1-w)\cdot \underbrace{l(X)}_{\text{the stable component}} \\ + w \cdot \underbrace{\frac{1-e^{-\lambda}}{1-e^{-\lambda(t-1)}} \left( \sum_{i=1}^{t-1} e^{-\lambda(i-1)} \cdot \delta(X - \mathbb{E}_{t-i}[\tilde{X}_{t-i}|R_{x,t-i}]) \right)}_{\text{the fast-moving component}} \end{array} \right\}, \tag{22}$$

where $w$ is the overall weight the $DM$ puts on the perceived values of $X$ observed in the recent environment, $\delta(\cdot)$ is a standard Dirac delta function, and the parameter $\lambda$ controls the relative weights the $DM$ assigns to the past perceived values of $X$ she has observed. The perceived value of $X$ from $i$ periods ago, $\mathbb{E}_{t-i}[\tilde{X}_{t-i}|R_{x,t-i}]$ receives a weight of $[(1-e^{-\lambda})/(1-e^{-\lambda(t-1)})]e^{-\lambda(i-1)}$. Thus, the more recent perceived value is assigned a higher weight, which is consistent with a large literature on memory recall showing that the probability of recalling a given value is based, in part, on its temporal similarity to the current value (Kahana (2012) and Bordalo et al. (2019)).[18] We also assume that the $DM$'s prior belief about $C$ is formed using a similar definition to that in (22):

$$f(C;\lambda) = \left\{ \begin{array}{c} (1-w)\cdot l(C) \\ + w \cdot \frac{1-e^{-\lambda}}{1-e^{-\lambda(t-1)}} \left( \sum_{i=1}^{t-1} e^{-\lambda(i-1)} \cdot \delta(C - \mathbb{E}_{t-i}[\tilde{C}_{t-i}|R_{c,t-i}]) \right) \end{array} \right\}. \tag{23}$$

To illustrate the implications of this adaptation model, we now assume a particular functional form for the stable components in equations (22) and (23), $l(X)$ and $l(C)$. As discussed earlier, Dehaene and Mehler (1992) present evidence that a monotonically decreasing distribution is a good approximation for the distribution of naturally occurring numbers (see also Stewart et al. (2006)). Therefore, we assume that $l(X)$ and $l(C)$ take the form of a gamma distribution

$$l(X) = \frac{1}{\Gamma(k)\theta^k} X^{k-1} e^{-X/\theta} \quad \text{and} \quad l(C) = \frac{1}{\Gamma(k)\theta^k} C^{k-1} e^{-C/\theta}, \tag{24}$$

where $\Gamma(\cdot)$ is the gamma function, and we set the parameter values for $\theta$ and $k$ such that the gamma distribution is monotonically decreasing.

[18] Moreover, the weighting scheme proposed in equation (22) is consistent with the notion of interference studied in the memory literature, whereby memories with greater temporal similarity to the current cue block the recall of memories with less temporal similarity (Kahana (2012)).

Equation (7) in Proposition 1 now implies the following likelihood functions

$$
\begin{aligned}
f(R_x|X,\lambda) &= \frac{1}{\sqrt{2\pi}\cdot\sigma}\exp\left(-\frac{(F(X;\lambda)-R_x)^2}{2\sigma^2}\right),\\
f(R_c|C,\lambda) &= \frac{1}{\sqrt{2\pi}\cdot\sigma}\exp\left(-\frac{(F(C;\lambda)-R_c)^2}{2\sigma^2}\right),
\end{aligned}
\tag{25}
$$

where $F(X;\lambda)$ and $F(C;\lambda)$ are the cumulative density functions of $f(X;\lambda)$ and $f(C;\lambda)$ from equations (22) and (23), respectively. We can then use the likelihood functions in (25) and the prior beliefs in (22) and (23) to obtain the posterior estimates of $X$ and $C$ at each time $t$, $\mathbb{E}_t[\tilde{X}_t|R_{x,t}]$ and $\mathbb{E}_t[\tilde{C}_t|R_{c,t}]$. As in the static model, the $DM$ chooses the risky lottery over the certain option if and only if $p\cdot\mathbb{E}_t[\tilde{X}_t|R_{x,t}]$ is greater than $\mathbb{E}_t[\tilde{C}_t|R_{c,t}]$.

### *2. Model's implications*

We now examine how a subject in our risky choice experiment would behave if, at each time $t$, she forms prior beliefs about the distributions of $X$ and $C$ according to our model of adaptation. In particular, we focus on whether a subject would still exhibit a systematic increase in her sensitivity to payoffs in the low volatility condition, compared to the high volatility condition.

We proceed by simulating data from the dynamic model, using parameters from our experimental design. Specifically, we simulate data from a single "pseudo-subject" who chooses between the risky lottery and the certain option on each trial over a series of 300 blocks that alternate between the high volatility and low volatility conditions; each block contains 60 trials from a given volatility condition. On each trial, the values of $X$ and $C$ are drawn from the joint lognormal distribution specified in (19).

We emphasize that, in contrast to the static model, here the subject is not endowed with the true stimulus distributions as her prior beliefs at the beginning of each block. Instead, the subject uses a set of past perceived payoffs to form her prior beliefs. These prior beliefs then generate a set of likelihood functions through efficient coding, and together, they allow the subject to form posterior estimates of the true payoffs.

In addition to the parameter values that specify the payoff distributions of $X$ and $C$ from the risky choice experiment, we also set values for "belief-based" parameters from equations (22), (23),

and (24). First, we specify the value of $\lambda$. This parameter controls the length of the "lookback window:" when $\lambda$ is high, only a short history of past perceived payoffs affects the subject's prior belief about the current payoff. Here, we set $\lambda = 0.154$: this value means that the subject uses approximately the last 15 trials to form her prior belief, with more weight assigned to more recent perceived payoffs. Next, we set the parameters of the gamma distribution, $\theta$ and $k$, to 40 and 0.5, respectively. These two values guarantee that the stable component of the subject's prior belief is monotonically decreasing, in accordance with the evidence from Dehaene and Mehler (1992). Finally, we set $w = 0.5$, so that the subject's prior belief on each trial is equally split between the stable component and the fast-moving component.

For this set of parameter values, we run a logistic regression on the simulated data using the model specification in equation (20). We find that the coefficient on the interaction term, $\ell\text{n}(X/C) \times \textit{high}$, is negative. This regression result confirms that, in a model of efficient coding where the $DM$'s prior beliefs adapt using perceived values, risk taking remains more sensitive to payoff values in the low volatility condition, compared to the high volatility condition.

It is worth noting that this model prediction does *not* hold for all parameter values. In particular, when $w = 1$, the subject's prior belief is completely driven by the local context. Somewhat paradoxically, this complete reliance on local context causes adaptation to cease in our model. To understand this result, first notice that, in the absence of the stable component of the prior belief that assigns probability density over a wide range of payoff values, the $DM$'s perceived value of an outlier payoff tends to be significantly biased toward the mean of the prior distribution. Given that the $DM$ can only learn from perceived values, this type of biased perception is self-fulfilling: the prior belief becomes more concentrated over time until it becomes completely degenerate.

A direct consequence of a degenerate prior is that perception—and therefore risk taking—becomes insensitive to payoff values. Since risk taking does not vary across volatility conditions, our main model prediction breaks down when $w = 1$. This finding of "insufficient learning" is consistent with Gagnon-Bartsch, Rabin, and Schwartzstein (2018), who argue that mistaken beliefs may persist because agents channel their attention through the lens of their mistaken beliefs, and therefore, ignore objectively useful information that they *believe* is irrelevant.

# VI. Discussion

## 1. *Definition of efficiency*

In our model, we assume that the encoding process is efficient in the sense that the $DM$ maximimizes the mutual information between the true payoff value and its noisy representations. This definition of efficiency is taken from recent work in theoretical neuroscience (Wei and Stocker (2015)). We choose to maintain this assumption in our model because ($i$) it generates predictions that closely match choice data in both perceptual and economic experiments (Polania et al. (2019)), and ($ii$) the framework of Wei and Stocker (2015) provides a simple procedure that allows us to derive the likelihood functions from *any* continuous prior distribution.

However, alternative definitions of efficient coding are plausible. For example, one alternative definition is that the $DM$ encodes payoffs in the choice set to maximize the expected financial gain on each trial. This type of objective is closer in spirit to models of rational inattention (Sims (2003); Sims (2011)) and models of inattentive valuation (Woodford (2012a,b)), in which the $DM$ chooses a signal structure that maximizes expected utility.

Our two laboratory experiments were not designed to distinguish between the hypotheses of maximizing mutual information and maximizing the expected financial gain. As such, it is possible that allocating coding resources toward frequently occurring payoffs could serve to maximize the expected financial gain in both of our experiments. To provide a cleaner test between the two hypotheses, we conducted a third experiment that was identical to the perceptual experiment discussed in Section IV, except that we slightly altered the incentive structure. Specifically, we paid subjects *only* for those trials where $X$ was in the range $[51, 79]$. We chose this range so that it coincides exactly with the range of the low volatility distribution.[19]

In this design, the distribution of numbers still varies across the two volatility conditions, but crucially, the distribution of *payoff-relevant* numbers is held constant across conditions. Therefore, if subjects allocate perceptual resources with the objective to maximize the expected financial gain, then perceptual resources should not adjust across the two volatility conditions. This in turn implies that classification accuracy in the payoff-relevant range, $[51, 79]$, should be identical across the two conditions. Instead, if subjects allocate perceptual resources to maximimize mutual information,

[19] More details on experimental procedures are given in Appendix C.

then classification should be more sensitive to numbers in the low volatility condition compared to the high volatility condition.

Figure C1 in Appendix C shows that, for this third experiment, classification among numbers in the payoff-relevant range continues to be more accurate in the low volatility condition, compared to the high volatility condition. Thus, the presence of unincentivized trials in the high volatility condition—those in which $X$ falls outside the payoff-relevant range of $[51, 79]$—has a systematic impact on the perception of numbers on incentivized trials. Our finding suggests that in our simple perceptual experiments, coding resources are allocated in a manner that is consistent with maximization of mutual information between the true stimulus value and its noisy signal—even if the true stimulus value is not directly payoff-relevant.[20]

### *2. Comparing our encoding functions with the KLW encoding functions*

KLW show that within a specific class of logarithmic encoding functions, maximizing the expected financial gain implies a very similar prediction to the one obtained in our model, namely, that the sensitivity of risk taking to payoffs decreases in the volatility of the prior distribution.

However, we emphasize that a major difference between our model and KLW lies in the malleability of our encoding functions. Specifically, KLW assume logarithmic encoding functions, whereas the encoding functions in our model depend heavily on the shape of the prior distribution to which the $DM$ has adapted. Therefore, we can separate the predictions of the two models by assessing the impact of the prior distribution on the encoding functions.

As described in Section II.4, for a monotonically decreasing prior, both our model and KLW predict that the $DM$ encodes smaller stimulus values more accurately, and as a result, the predictions of the two models are similar.[21] However, for priors in which there is a greater chance of observing a larger stimulus value, KLW continue to predict that smaller stimulus values are encoded more accurately, while our model predicts that larger stimulus values are encoded more accurately.

[20] Clearly, our finding does not rule out the possibility that maximization of the expected financial gain is also an important determinant of coding resources.

[21] Because a monotonically decreasing prior assigns higher probability density to smaller values compared to larger values, efficient coding implies that smaller values are encoded more precisely. Therefore, our model generates a set of encoding functions that resemble the logarithmic encoding functions assumed in KLW. This offers an alternative interpretation for some of the experimental results in KLW. In their experimental design, KLW sample payoff values from a distribution that is approximately monotonically decreasing for both $X$ and $C$ (this is because, by design, the distance between successive payoffs is increasing in the magnitude of the payoffs). In such an experiment, our model would thus predict that the encoding functions should be similar to the ones assumed in KLW.

Although the latter prediction stands in stark contrast to Weber's law, recent experimental work from Polania et al. (2019) provides evidence that there is indeed less variability in the subjective ratings of high value food items, compared to low value food items. The authors interpret this empirical pattern as arising from efficient coding and a particular prior distribution of food items that has a high expected value. They also make the important observation that such an empirical pattern does not invalidate Weber's law. Instead, it suggests that the strength of Weber's law depends on the prior distribution to which the $DM$ has adapted.[22]

### *3. Probability weighting*

Throughout the paper, we have assumed that the $DM$ perceives probabilities without any noise. In reality, there is likely to be noisy encoding of both payoffs and probabilities. Our model of efficient coding also has direct implications for the perception of probability. For any distribution of probability, $f(p)$, the efficient coding condition in (6) implies that the likelihood function is

$$f(R_p|\, p) = \frac{1}{\sqrt{2\pi}\cdot\sigma} exp\left(-\frac{(F(p)-R_p)^2}{2\sigma^2}\right), \tag{26}$$

where $F(p) = \int_0^p f(\xi)d\xi$ is the cumulative density function of $f(p)$. Moreover, following the discussion in Section II.4, we define the probability weighting function of $p$ and the standard deviation of this probability weighting function as

$$\begin{aligned} \pi(p) &= \int_{-\infty}^{\infty} \mathbb{E}[\tilde{p}|R_p] f(R_p|\, p) dR_p, \\ \sigma(p) &= \left[\int_{-\infty}^{\infty} \left(\mathbb{E}[\tilde{p}|R_p]\right)^2 f(R_p|\, p) dR_p - \pi^2(p)\right]^{1/2}, \end{aligned} \tag{27}$$

where

$$\mathbb{E}[\tilde{p}|R_p] = \frac{\int_0^1 f(R_p|\, p) f(p) p dp}{\int_0^1 f(R_p|\, p) f(p) dp}. \tag{28}$$

In the context of prospect theory (Kahneman and Tversky (1979); Tversky and Kahneman (1992)), the probability weighting function $\pi(p)$ in (27) is interpreted as the decision weight associated with

[22] In Appendix B, we provide further analyses of our model's implications for Weber's law and the "scale invariance" of risk taking.

probability $p$.

**[Place Figure 9 about here]**

To illustrate our model's implications for the perception of probability, Figure 9 presents a numerical example. We assume a particular distribution of probability that is motivated by the frequency of probabilities used in experiments and in natural language. In particular, Stewart et al. (2006) make the observations that: $(i)$ small and large probabilities occur more frequently than mid-range probabilities; and $(ii)$ large probabilities occur more frequently than small probabilities. Given a distribution of probabilities, $f(p)$, that is consistent with these observations, Figure 9 shows that the implied probability weighting function $\pi(p)$ gives rise to both the overweighting of small probabilities—that is, $\pi(p) > p$ when $p$ is close to zero—and the asymmetry in $\pi(\cdot)$—that is, $\pi(0.5) < 0.5$. Both are important features of the probability weighting function in prospect theory (Tversky and Kahneman (1992)). To the extent that extreme outcomes tend to be associated with small probability events, our model also helps explain the overweighting of extreme outcomes (Bordalo, Gennaioli, and Shleifer (2012)).

### *4. A comparison with salience theory*

Here we compare our model with salience theory, an alternative model of risky choice that is also grounded in principles of perception (Bordalo et al. (2012)). Under salience theory, attention is drawn to those payoffs that are very different in percentage terms from a precisely defined reference payoff. Bordalo et al. (2012) appeal to Weber's law of diminishing sensitivity—in part—as a justification for their definition of salience. Importantly, in their model, Weber's law is an exogenous assumption. In contrast, Weber's law arises endogenously in our model: efficient coding implies that coding resources are often allocated toward the average payoff, and as a result, the $DM$ cannot easily discriminate between stimuli that are in a tail of the prior distribution. In this sense, salience theory and efficient coding differ with respect to their primitive assumptions.

Naturally, this leads the two models to generate distinct predictions in many environments. For example, salience theory rationalizes the Allais paradox, in which the $DM$ reverses her choice between two lotteries as a function of a common consequence (Allais (1953)). Salience theory also helps explain the dependence of risk taking on the correlation between mutually exclusive lotteries.

Our model, in its current form, does not generate these predictions. Another difference between the two models revolves around stochastic choice. A central ingredient of our model is stochastic perception, which leads to stochastic choice. Salience theory, in contrast, predicts only deterministic choice.

There are also some environments in which the two models give rise to similar predictions. For example, in the simple risky choice experiment that we conducted with a single risky lottery and a certain option, both efficient coding and salience theory can explain the basic features of our data. Figure D2 shows that the probability of risk taking is a strong positive function of the difference in the salience implied lottery valuations. The figure also shows that one dimension of our experimental data that salience theory cannot explain is the dependence of risk taking on the recently encountered distribution of payoffs.[23] In Appendix D, we provide a more comprehensive comparison between the two theories in the context of our simple risky choice experiment.

### *5. Limitations of the model*

In this subsection, we discuss three limitations of our model in addressing richer information structures and some documented patterns of choice under risk. First, in our model, the $DM$ forms perceptions of $X$ and $C$ separately, even though there is a positive correlation between these two payoffs in our experimental design. If one allows the $DM$ to jointly form perceptions of $X$ and $C$, this would significantly enrich the space of possible encoding functions. Specifically, the encoding function governing the distribution of $R_x$ could depend on both $X$ and $C$. Analyzing the predictions of such a multidimensional efficient code is an important direction for future research.

Second, the model we presented in Section II does not predict some of the classic patterns in choice under risk. For example, when the $DM$ efficiently codes payoffs—but not probabilities—our model would not predict the Allais paradox or a preference for positively skeweed lotteries. Prospect theory generates these effects through the overweighting of small probabilities, whereas regret theory and salience theory rely on the overweighting of payoffs in states in which there are large payoff differences (Loomes and Sugden (1982); Bordalo et al. (2012)). The efficient coding

[23] A natural way to incorporate this dependence is to allow the salience function defined in Bordalo et al. (2012) to depend on past payoffs. This is in the spirit of a more recent version of salience theory, in which memory of past experiences shapes perception of the current choice set (Bordalo et al. (2019)). However, the model of Bordalo et al. (2019) focuses mainly on riskless choice, whereas our model focuses on risky choice.

of probability that we presented in Section VI.3 does generate overweighting of small probabilities, and therefore offers a promising direction for explaining the Allais paradox and a preference for positive skewness through a noisy coding mechanism. Yet it remains unclear precisely how efficient coding of payoffs and probabilities interact. An obvious next step in this direction is to conduct experiments in which the joint distribution of payoffs and probabilities is manipulated across blocks.

A third limitation of our model is that we only consider a simple risky choice environment with a single risky lottery and a certain option. In this environment, the correlation between lotteries—that is, the correlation between the marginal distributions of lottery payoffs—is zero by construction. However, in a more complex environment with at least two risky lotteries, experimental evidence indicates that the correlation between lotteries does affect risky choice (Loomes and Sugden (1987); Bordalo et al. (2012); Frydman and Mormann (2018); Dertwinkel-Kalt and Köster (2019)). Therefore, one could extend our model to potentially explain this sensitivity to correlation by allowing the $DM$ to allocate her overall coding capacity across multiple attributes. In this regard, Woodford (2012b) shows that when all attributes have a Gaussian distribution, the $DM$ efficiently allocates more resources to attributes that are associated with a wider range. Because the correlation between lotteries affects the payoff range along each attribute, correlation may also affect the capacity assigned to each attribute. More work is needed to understand these implications, particularly for more general, non-Gaussian distributions of attribute values.

# VII. Conclusion

In this paper, we derive the implications for risk taking when the perception of payoffs is noisy and governed by efficient coding. We show that the $DM$'s value function is malleable, and its shape fluctuates with the distribution of recent payoffs. In particular, because the $DM$ has difficulty discriminating between those payoffs that do not occur frequently, efficient coding generates diminishing sensitivity, which itself can change across environments. To test our model, we conduct two laboratory experiments in which we find evidence consistent with efficient coding of risky payoffs. Specifically, risk taking becomes more sensitive to those payoffs that appear more frequently in the choice set. In our second experiment, where subjects only need to classify whether a symbolic number is larger than a reference level, we find that classification accuracy systematically

changes with the distribution of recently observed numbers.

We also provide a dynamic extension of our model, which explicitly incorporates the adaptation process across experimental trials. We find that for some parameter values, even when the $DM$ can only update her prior beliefs based on perceived past payoffs, the model continues to predict that risk taking is more sensitive to payoffs in the low volatility condition. However, there are several other questions regarding dynamics that are important to address in future research.

For example, if the $DM$ can only learn from perceived values, under what conditions will her beliefs converge to the true distribution? The answer to this question will likely depend on the number of signals the $DM$'s perceptual system draws when presented with a single stimulus. For simplicity, our model assumes that only one noisy signal is drawn from the $DM$'s likelihood function. However, the literature on sequential sampling models suggests that the number of signals drawn may itself depend on the precision of the $DM$'s likelihood function (Ratcliff (1978); Krajbich, Armel, and Rangel (2010); Woodford (2014)). Therefore, incorporating additional constraints on information sampling within a trial is another important direction for future research on efficient coding.

# REFERENCES


Allais, Maurice, 1953, Le comportement de l'homme rationnel devant le risque: critique des postulats et axiomes de l'ecole americaine, *Econometrica* 21, 503–546.

Barberis, Nicholas, 2013, Thirty years of prospect theory in economics: A review and assessment, *Journal of Economic Perspectives* 27, 173–196.

Barberis, Nicholas, 2018, Psychology-based models of asset prices and trading volume, in Douglas Bernheim, Stefano DellaVigna, and David Laibson, eds., *Handbook of Behavioral Economics* (North Holland, Amsterdam).

Barlow, Horace, 1961, Possible principles underlying the transformations of sensory messages, in Walter A. Rosenblith, ed., *Sensory Communication*, 217–234 (MIT Press).

Bhui, Rahul, and Samuel Gershman, 2018, Decision by sampling implements efficient coding of psychoeconomic functions, *Psychological Review* 125, 985–1001.

Bordalo, Pedro, Nicola Gennaioli, and Andrei Shleifer, 2012, Salience theory of choice under risk, *Quarterly Journal of Economics* 127, 1243–1285.

Bordalo, Pedro, Nicola Gennaioli, and Andrei Shleifer, 2019, Memory, attention, and choice, Working paper.

Burke, Christopher J., Michelle Baddeley, Philippe N. Tobler, and Wolfram Schultz, 2016, Partial adaptation of obtained and observed value signals preserves information about gains and losses, *Journal of Neuroscience* 36, 10016–10025.

Bushong, Benjamin, Matthew Rabin, and Joshua Schwartzstein, 2017, A model of relative thinking, Working paper.

Carandini, Matteo, and David J. Heeger, 2012, Normalization as a canonical neural computation, *Nature Reviews Neuroscience* 13, 51–62.

Conen, Katherine E., and Camillo Padoa-Schioppa, 2019, Partial adaptation to the value range in the macaque orbitofrontal cortex, *Journal of Neuroscience* 39, 3498–3513.

Dehaene, Stanislas, 1992, Varieties of numerical abilities, *Cognition* 44, 1–42.

Dehaene, Stanislas, 2011, *The Number Sense* (Oxford University Press, Oxford, United Kingdom).

Dehaene, Stanislas, Emmanuel Dupoux, and Jacques Mehler, 1990, Is numerical comparison digital? analogical and symbolic effects in two-digit number comparison, *Journal of Experimental Psychology: Human Perception and Performance* 16, 626–641.

Dehaene, Stanislas, and Jacques Mehler, 1992, Cross-linguistic regularities in the frequency of number words, *Cognition* 43, 1–29.

Dertwinkel-Kalt, Markus, and Mats Köster, 2019, Salience and skewness preferences, *Journal of the European Economic Association* forthcoming.

Frydman, Cary, and Milica Milosavljevic Mormann, 2018, The role of salience in choice under risk: An experimental investigation, SSRN working paper.

Gabaix, Xavier, and David Laibson, 2017, Myopia and discounting, NBER working paper No. 23254.

Gagnon-Bartsch, Tristan, Matthew Rabin, and Joshua Schwartzstein, 2018, Channeled attention and stable errors, Working paper.

Girshick, Ahna R., Michael S. Landy, and Eero P. Simoncelli, 2011, Cardinal rules: Visual orientation perception reflects knowledge of environmental statistics, *Nature Neuroscience* 14, 926–932.

Halberda, Justin, Michele Mazzocco, and Lisa Feigenson, 2008, Individual differences in non-verbal number acuity correlate with maths achievement, *Nature* 445, 665–668.

Imas, Alex, 2016, The realization effect: Risk-taking after realized versus paper losses, *American Economic Review* 106, 2086–2109.

Kahana, Michael, 2012, *Foundation of Human Memory* (Oxford University Press, Oxford, United Kingdom).

Kahneman, Daniel, and Amos Tversky, 1979, Prospect theory: An analysis of decision under risk, *Econometrica* 47, 263–291.

Khaw, Mel Win, Paul W. Glimcher, and Kenway Louie, 2017, Normalized value coding explains dynamic adaptation in the human valuation process, *Proceedings of the National Academy of Sciences* 114, 12696–12701.

Khaw, Mel Win, Ziang Li, and Michael Woodford, 2019, Cognitive imprecision and small-stakes risk aversion, NBER working paper No. 24978.

Krajbich, Ian, Carrie Armel, and Antonio Rangel, 2010, Visual fixations and the computation and comparison of value in simple choice, *Nature Neuroscience* 13, 1292–1298.

Kutter, Esther, Jan Bostroem, Christian Elger, Florian Mormann, and Andreas Nieder, 2018, Single neurons in the human brain encode numbers, *Neuron* 100, 1–9.

Landry, Peter, and Ryan Webb, 2018, Pairwise normalization: A neuroeconomic theory of multi-attribute choice, SSRN working paper.

Laughlin, Simon, 1981, A simple coding procedure enhances a neuron's information capacity, *Zeitschrift fur Naturforschung* 36, 9–10.

Loomes, Graham, and Robert Sugden, 1982, Regret theory: An alternative theory of rational choice under uncertainty, *The Economic Journal* 92, 805–824.

Loomes, Graham, and Robert Sugden, 1987, Testing for regret and disappointment in choice under uncertainty, *The Economic Journal* 97, 118–129.

Louie, Kenway, and Paul W. Glimcher, 2012, Efficient coding and the neural representation of value, *Annals of the New York Academy of Sciences* 1251, 13–32.

Moyer, Robert S., and Thomas K. Landauer, 1967, Time required for judgments of numerical inequality, *Nature* 215, 1519–1520.

Padoa-Schoppa, Camillo, 2009, Range-adapting representation of economic value in the orbitofrontal cortex, *Journal of Neuroscience* 29, 14004–14014.

Payzan-LeNestour, Elise, and Michael Woodford, 2019, 'outlier blindness': Efficient coding generates an inability to represent extreme values, SSRN working paper.

Polania, Rafael, Michael Woodford, and Christian Ruff, 2019, Efficient coding of subjective value, *Nature Neuroscience* 22, 134–142.

Rangel, Antonio, and John A. Clithero, 2012, Value normalization in decision making: Theory and evidence, *Current Opinion in Neurobiology* 22, 970–981.

Ratcliff, Roger, 1978, A theory of memory retrieval, *Psychological Review* 85, 59–108.

Robson, Arthur J., and Lorne A. Whitehead, 2018, Adaptive hedonic utility, Working paper.

Sims, Christopher A., 2003, Implications of rational inattention, *Journal of Monetary Economics* 50, 665–690.

Sims, Christopher A., 2011, Rational inattention and monetary economics, in Benjamin M. Friedman, and Michael Woodford, eds., *Handback of Monetary Economics,* (Amsterdam: Elsevier).

Soltani, Alireza, Benedetto De Martino, and Colin Camerer, 2012, A range-normalization model of context-dependent choice: A new model and evidence, *PLoS Computational Biology* 8, e1002607.

Steiner, Jakub, and Colin Stewart, 2016, Perceiving prospects properly, *American Economic Review* 106, 1601–1631.

Stewart, Neil, Nick Chater, and Gordon Brown, 2006, Decision by sampling, *Cognitive Psychology* 53, 1–26.

Stocker, Alan A., and Eero P. Simoncelli, 2006, Noise characteristics and prior expectations in human visual speed perception, *Nature Neuroscience* 9, 578–585.

Thaler, Richard, and Eric Johnson, 1990, Gambling with the house money and trying to break even: The effects of prior outcomes on risky choice, *Management Science* 36, 643–660.

Tobler, Philippe N., Christopher D. Fiorillo, and Wolfram Schultz, 2005, Adapting coding of reward value by dopamine neurons, *Science* 307, 1642–1645.

Tversky, Amos, and Daniel Kahneman, 1992, Advances in prospect theory: Cumulative representation of uncertainty, *Journal of Risk and Uncertainty* 5, 297–323.

Tymula, Agnieszka, and Paul W. Glimcher, 2017, Expected subjective value theory (ESVT): A representation of decision under risk and certainty, SSRN working paper.

Weber, Martin, and Colin Camerer, 1998, The disposition effect in securities trading: An experimental analysis, *Journal of Economic Behavior and Organization* 33, 167–184.

Wei, Xue-Xin, and Alan A. Stocker, 2015, A bayesian observer model constrained by efficient coding can explain 'anti-bayesian' percepts, *Nature Neuroscience* 18, 1509–1517.

Wei, Xue-Xin, and Alan A. Stocker, 2016, Mutual information, fisher information, and efficient coding, *Neural Computation* 28, 305–326.

Wei, Xue-Xin, and Alan A. Stocker, 2017, Lawful relation between perceptual bias and discriminability, *Proceedings of the National Academy of Sciences* 114, 10244–10249.

Woodford, Michael, 2012a, Inattentive valuation and reference-dependent choice, Working paper.

Woodford, Michael, 2012b, Prospect theory as efficient perceptual distortion, *American Economic Review Papers and Proceedings* 102, 41–46.

Woodford, Michael, 2014, Stochastic choice: An optimizing neuroeconomic model, *American Economic Review Papers and Proceedings* 104, 495–500.

Zimmermann, Jan, Paul W. Glimcher, and Kenway Louie, 2018, Multiple timescales of normalized value coding underlie adaptive choice behavior, *Nature Communications* 9, 3206.

## Figure 1. Likelihood functions and the underlying stimulus distributions

The upper graphs plot two lognormal stimulus distributions of $X$ (left: low volatility; right: high volatility). The lower graphs plot the likelihood functions implied by efficient coding (left: low volatility; right: high volatility), for five different values of the noisy signal, $R_x = 0.15$, 0.2, 0.5, 0.8, and 0.85. Here, we treat the likelihood function $f(R_x|X)$ as a function of $X$ for each value of $R_x$: we set $L(X|R_x) \equiv f(R_x|X)$. The parameter values are: $\sigma_x = 0.19$ (left), $\sigma_x = 0.55$ (right), $\mu_x = 3.05$, and $\sigma = 0.1$.

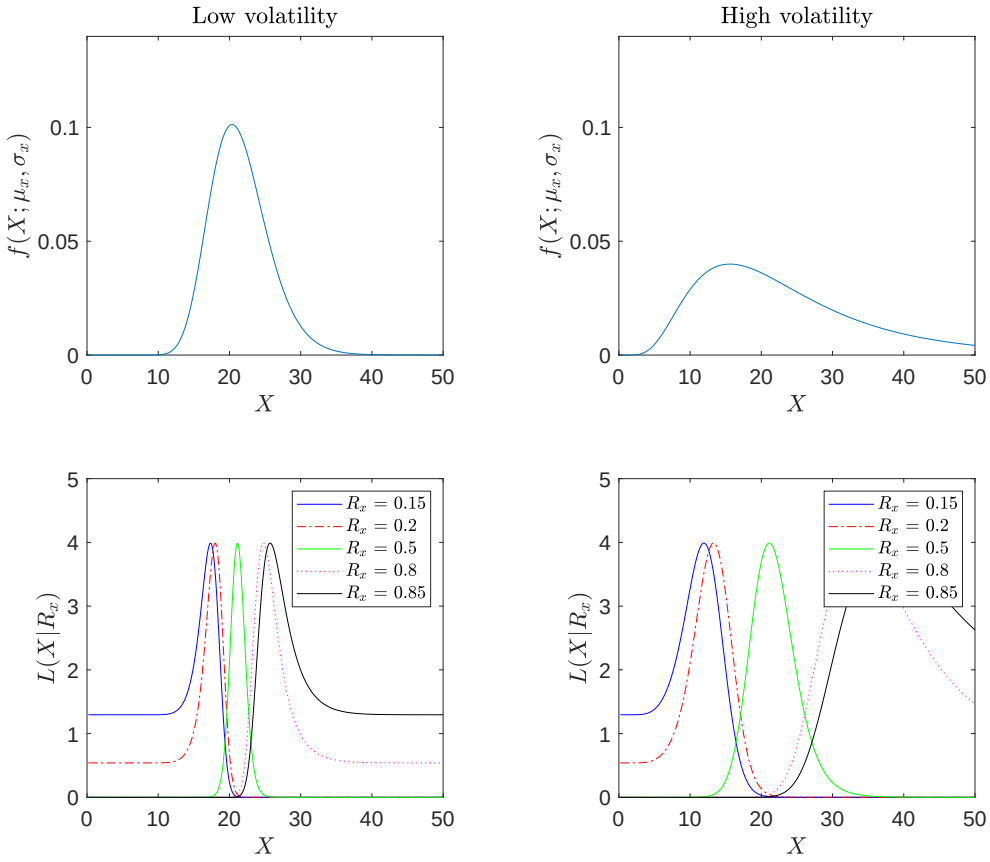

## Figure 2. Value functions and the underlying stimulus distribution

Panel A: the upper graph plots two lognormal stimulus distributions for $X$ (low volatility distribution in red is given by $\sigma_x = 0.19$; high volatility distribution in blue is given by $\sigma_x = 0.55$). The bottom graph plots the subjective value functions implied by efficient coding, $v(X)$, and their one-standard-deviation bounds $v(X) \pm \sigma(X)$. The other parameter values are: $\mu_x = 3.05$ and $\sigma = 0.1$. Panel B: the upper graph plots two monotonically decreasing stimulus distributions for $X$, which are characterized by a gamma distribution,

$$f(X; k, \theta) = \frac{1}{\Gamma(k)\theta^k} X^{k-1} e^{-X/\theta},$$

where $\Gamma(\cdot)$ is the gamma function (low volatility distribution in red is given by $\theta = 5$ and $k = 1$; high volatility distribution in blue is given by $\theta = 20$ and $k = 0.25$). The bottom graph plots the implied subjective value functions, $v(X)$, and their one-standard-deviation bounds $v(X) \pm \sigma(X)$. The other parameter value is: $\sigma = 0.1$. In the lower graphs of both panels, the green dash-dot line is the forty-five degree line.

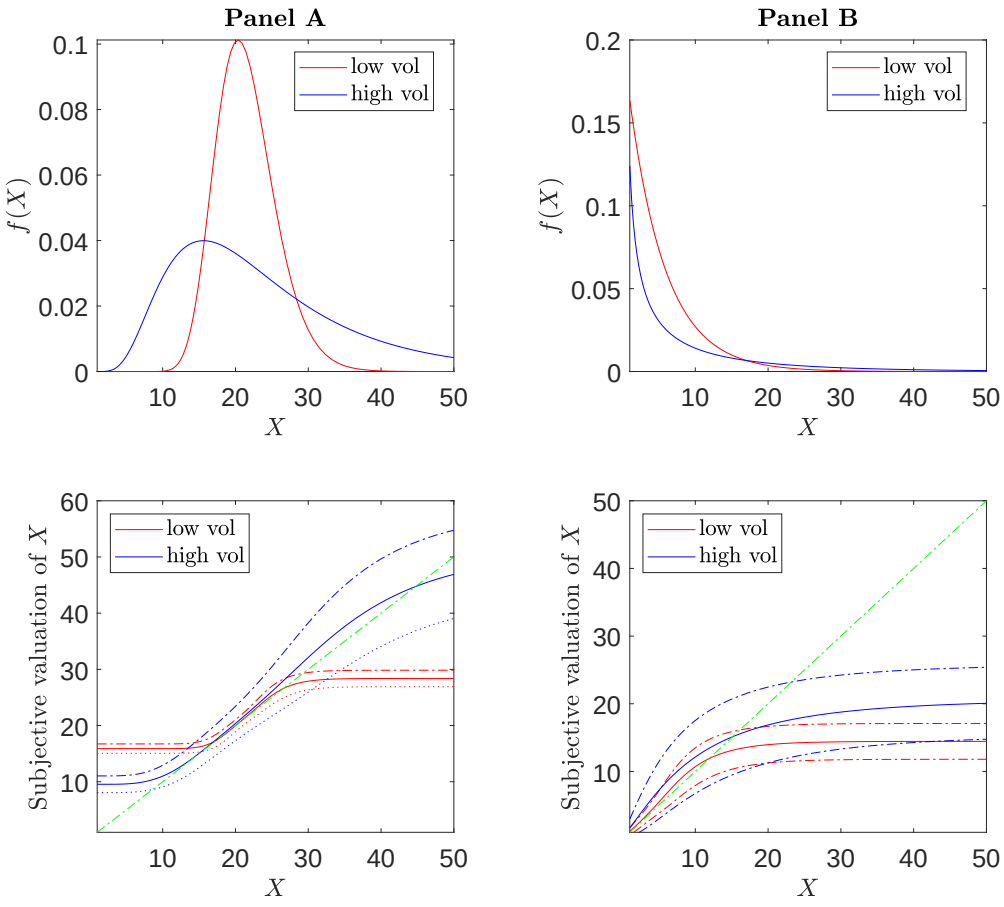

**Figure 3. Model predicted probability of choosing the risky lottery**

The figure plots, for each of three different volatility levels of the stimulus distribution, $\sigma_x = \sigma_c = 0.4$, 0.8, or 1.5, the probability of choosing the risky lottery computed from equation (18) of the main text. For each volatility level, we set $C$ to its mean value, $\exp(\mu_c + \frac{1}{2}\sigma_c^2)$, and vary the value of $X$. The other parameter values are: $\mu_x = 3.05$, $\mu_c = 2.35$, $p = 0.59$, and $\sigma = 0.1$.

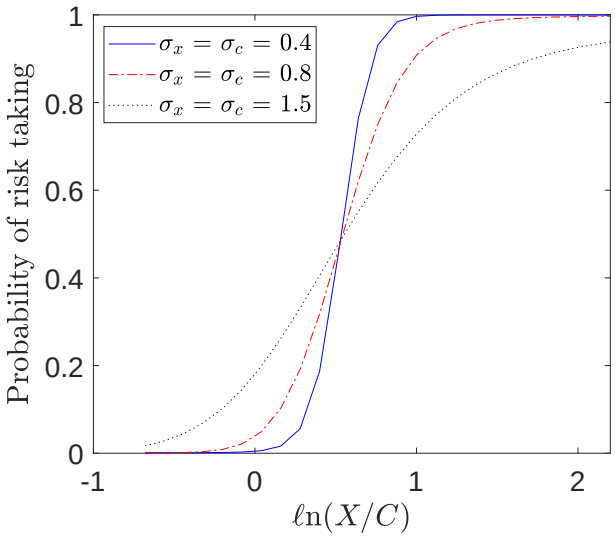

**Figure 4. Experimental design for the main task on risky choice**

The task consists of eight blocks, which alternated between a high volatility condition and a low volatility condition. In the example trial screenshot below, the risky lottery is shown on the left, and the certain option is shown on the right. In each trial, the subject has unlimited time to decide which of the two options she prefers. At the end of each block, the subject is allowed to take a self-paced break, after which the next block begins.

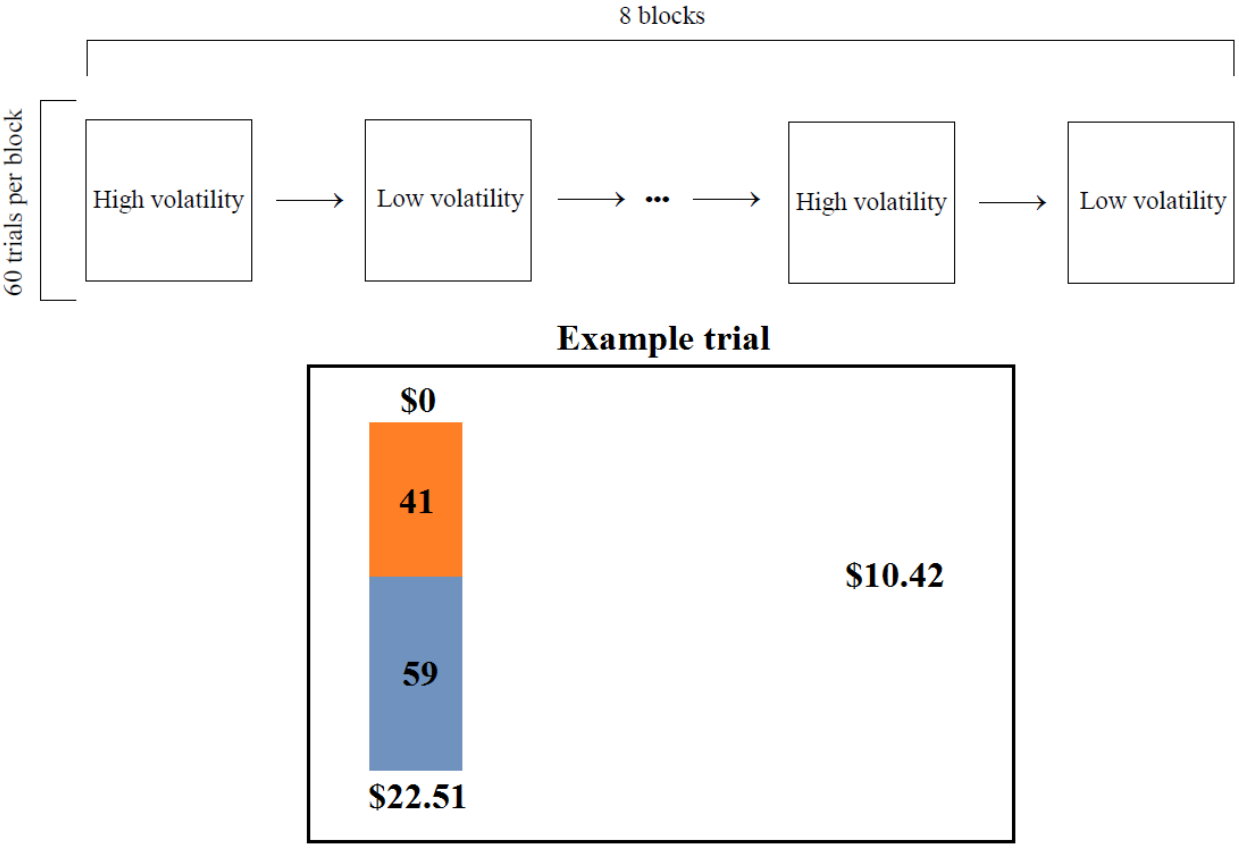

**Figure 5. Average levels of risk taking across conditions**

The figure plots the proportion of trials on which subjects choose the risky lottery as a function of $\ell n(X/C)$, for both the high volatility condition and the low volatility condition. Data are pooled across trials and subjects. For each of the two volatility conditions, we bin the $\ell n(X/C)$ variable into two-hundred bins such that each bin has an equal number of trials.

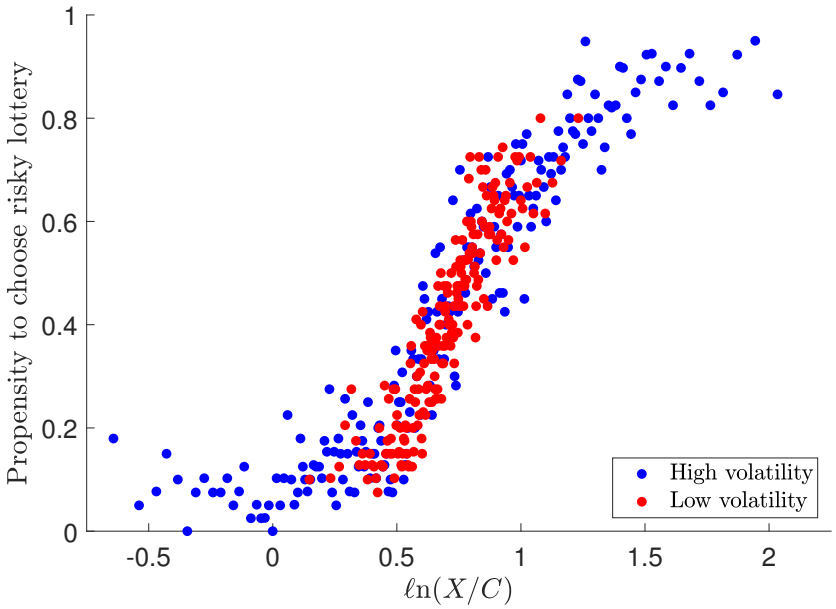

**Figure 6. Individual-level treatment effects from the main risky choice task**

For each subject, and each experimental condition, we run a logistic regression of the form: $\text{risky}_t = \alpha + \beta \cdot \ell\text{n}(X_t/C_t) + \varepsilon_t$. The $x$-axis measures the estimated $\beta$ in the high volatility condition, while the $y$-axis measures the estimated $\beta$ in the low volatility condition. Each point represents a single subject, and the length of each black bar denotes two standard errors of the mean. The blue line is the forty-five degree line.

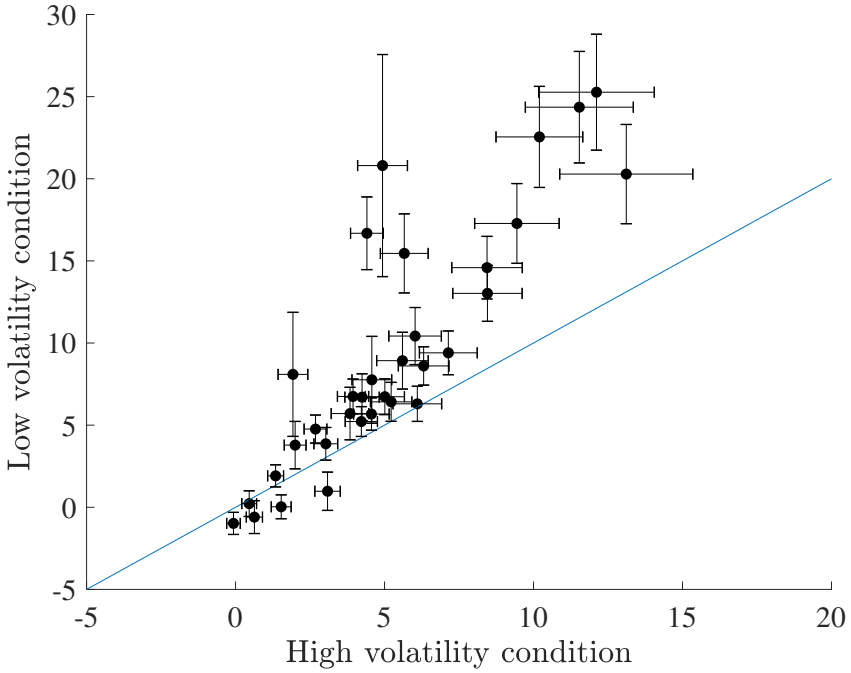

**Figure 7. Experimental design for the additional perceptual experiment**

The task consists of sixteen blocks, which alternated between a high volatility condition and a low volatility condition. On each trial, the subject is incentivized to classify, as quickly and accurately as possible, whether the stimulus integer is larger or smaller than the number 65. In the high volatility condition, the integers are drawn uniformly from $[31, 99]$, while in the low volatility condition, the integers are drawn uniformly from $[51, 79]$.

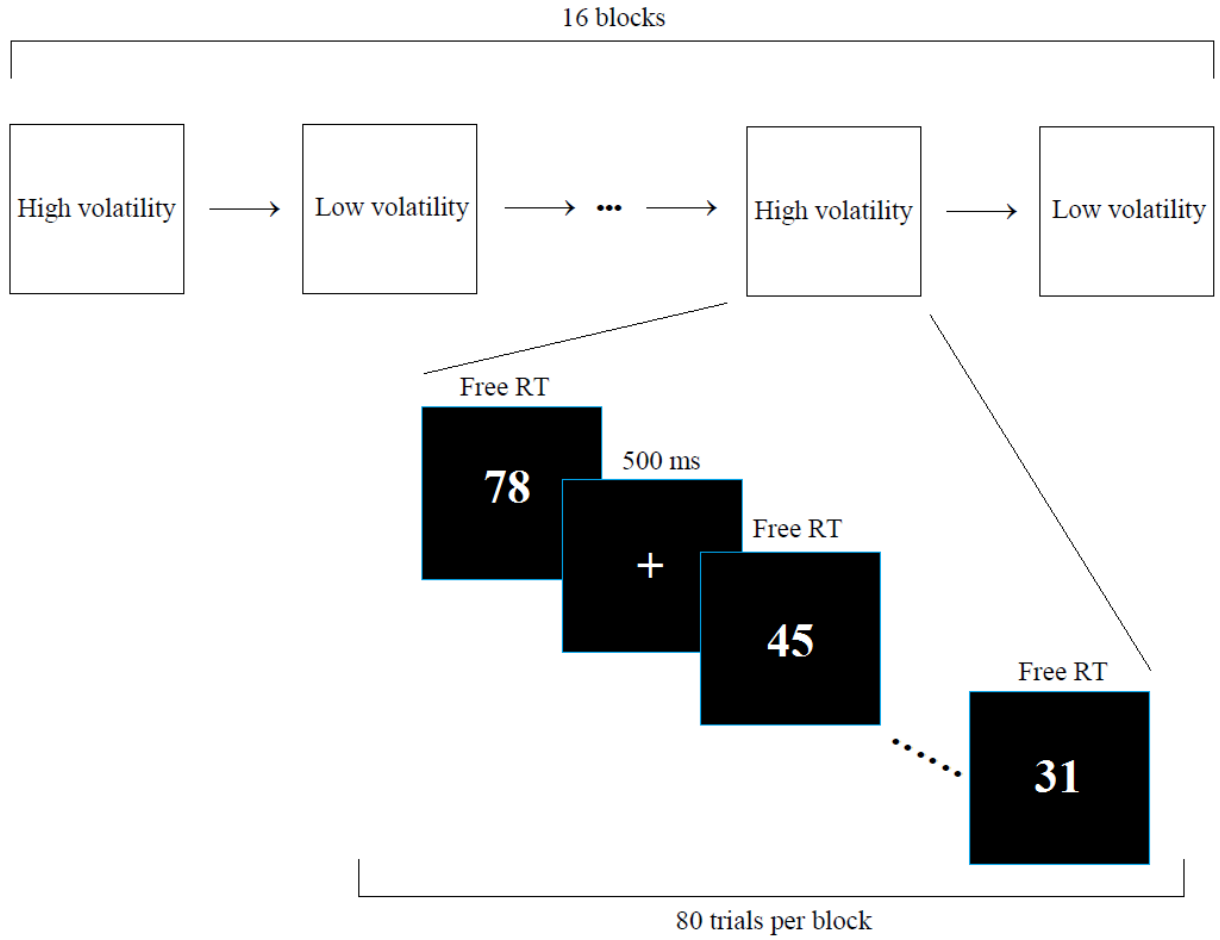

## Figure 8. Classification performance in the perceptual task

The $x$-axis denotes the integer $X$ that is presented on each trial. The $y$-axis denotes the proportion of trials for which subjects classified the integer $X$ as greater than 65. Data are pooled across trials and subjects, but are disaggregated by the high and low volatility conditions. In the high volatility condition, the integers are drawn uniformly from $[31, 99]$. In the low volatility condition, the integers are drawn uniformly from $[51, 79]$. Each subject was paid according to the accuracy and speed of her classifications. Specially, the incentive scheme is: Payout $= \$(20 \times accuracy - 10 \times avgseconds)$, where "*accuracy*" is the percentage of trials where the subject correctly classified $X$ as larger or smaller than 65, and "*avgseconds*" is the average amount of time it took the subject to classify a number throughout the experiment, in seconds.

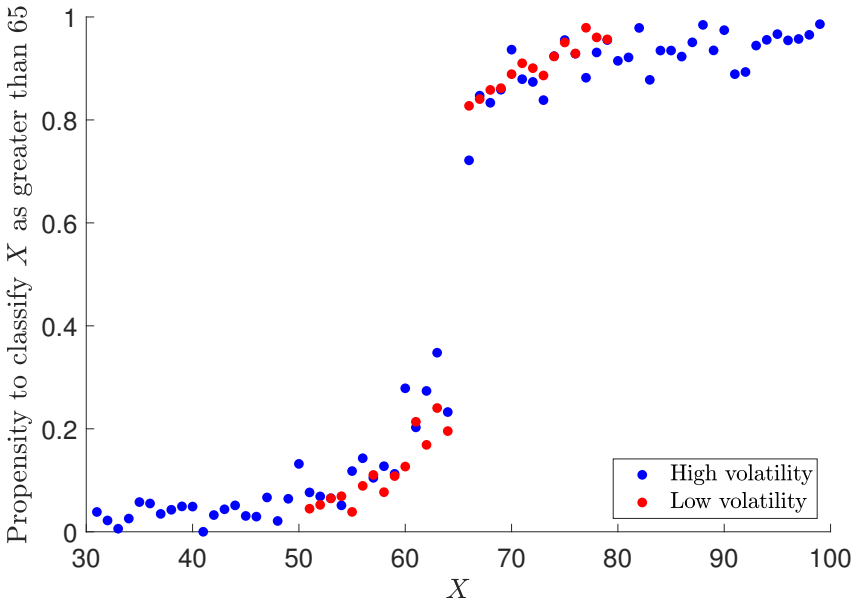

## Figure 9. Efficient coding of probability

The upper graph plots the following distribution of probability

$$f(p;\lambda_1,\lambda_2,w)=\frac{we^{-\lambda_1 p}+(1-w)e^{-\lambda_2(1-p)}}{(w/\lambda_1)(1-e^{-\lambda_1})+((1-w)/\lambda_2)(1-e^{-\lambda_2})}.$$

The bottom graph plots the implied probability weighting function, $\pi(p)$, and its one-standard-deviation bounds, $\pi(p)\pm\sigma(p)$. The parameter values are: $\lambda_1=7.5$, $\lambda_2=8.5$, $w=0.25$, and $\sigma=0.1$. The green dash-dot line is the forty-five degree line.

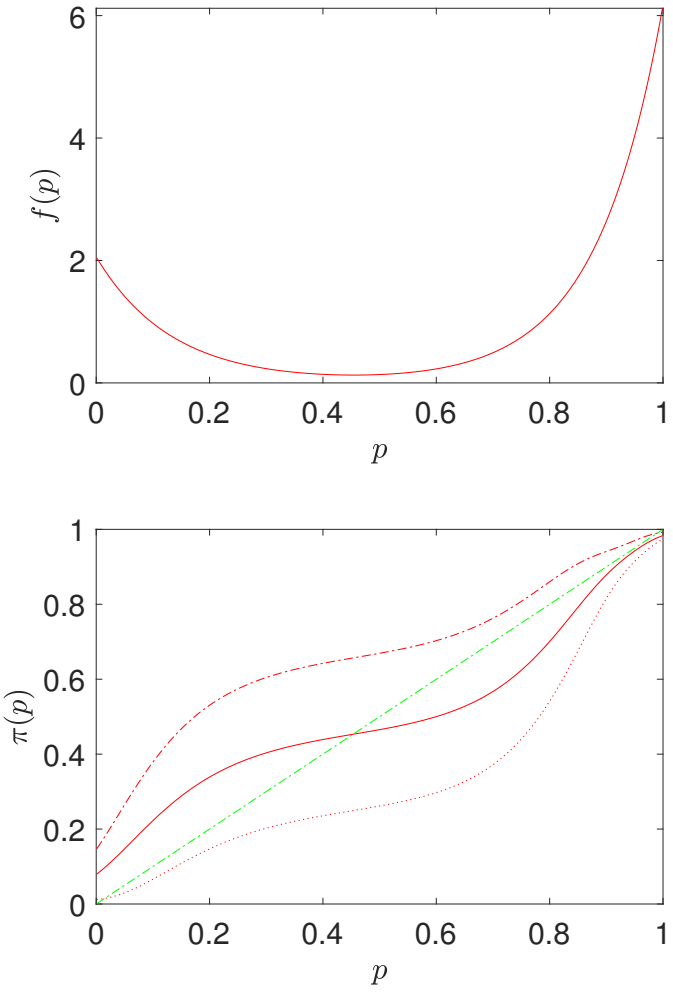

## Table 1. Probability of choosing the risky lottery

In both Panels A and B, we report results from logistic regressions where the dependent variable takes the value of one if the subject chose the risky lottery, and zero if the subject chose the certain option. The dummy variable *high* takes the value of one if the trial belongs to the high volatility condition, and zero if it belongs to the low volatility condition. Standard errors in parentheses are clustered at the subject level, and ***, **, * denote statistical significance at the 1%, 5%, and 10% levels, respectively.

### Panel A

| | (1) | (2) | (3) | (4) | (5) |
|---|---|---|---|---|---|
| Dependent variable: "Choose risky lottery" | All data | $0.02 < \ell\text{n}(X/C) < 1.36$ | First half of block | Second half of block | First 10 trials of each block |
| *high* | 0.99*** | 0.68*** | 0.84*** | 1.15*** | 1.10*** |
| | (0.28) | (0.26) | (0.30) | (0.32) | (0.29) |
| $\ell\text{n}(X/C)$ | 4.21*** | 4.21*** | 4.05*** | 4.37*** | 3.94*** |
| | (0.62) | (0.62) | (0.62) | (0.65) | (0.70) |
| $\ell\text{n}(X/C) \times high$ | –1.35*** | –0.92*** | –1.11*** | –1.59*** | –1.14*** |
| | (0.38) | (0.32) | (0.40) | (0.42) | (0.41) |
| Constant | –3.38*** | –3.38*** | –3.26*** | –3.51*** | –3.26*** |
| | (0.47) | (0.47) | (0.47) | (0.50) | (0.50) |
| Pseudo $R$-squared | 0.17 | 0.13 | 0.18 | 0.17 | 0.17 |
| Observations | 15,840 | 14,101 | 7,920 | 7,920 | 2,640 |

### Panel B

| | (1) | (2) | (3) | (4) |
|---|---|---|---|---|
| Dependent variable: "Choose risky lottery" | All data | First half of block | Second half of block | First 10 trials of each block |
| *high* | –0.10 | –0.20 | –0.01 | 0.03 |
| | (0.29) | (0.30) | (0.33) | (0.49) |
| $X$ | 0.18*** | 0.19*** | 0.17*** | 0.18*** |
| | (0.03) | (0.03) | (0.03) | (0.03) |
| $C$ | –0.41*** | –0.42*** | –0.41*** | –0.39*** |
| | (0.06) | (0.07) | (0.06) | (0.07) |
| $X \times high$ | –0.08*** | –0.09*** | –0.08*** | –0.07*** |
| | (0.02) | (0.02) | (0.02) | (0.03) |
| $C \times high$ | 0.18*** | 0.19*** | 0.16*** | 0.17*** |
| | (0.04) | (0.04) | (0.04) | (0.04) |
| Constant | 0.03 | –0.05 | 0.12 | –0.19 |
| | (0.42) | (0.43) | (0.45) | (0.53) |
| Pseudo $R$-squared | 0.15 | 0.15 | 0.15 | 0.15 |
| Observations | 15,840 | 7,920 | 7,920 | 2,640 |

## Table 2. Probability of classification in perceptual task

The table reports results from logistic regressions where the dependent variable takes the value of one if the subject classified the stimulus, $X$, as larger than 65, and zero otherwise. The dummy variable *high* takes the value of one if the trial belongs to the high volatility condition, and zero if it belongs to the low volatility condition. In the high volatility condition, the integer $X$ is drawn uniformly from $[31, 99]$, while in the low volatility condition, the integer is drawn uniformly from $[51, 79]$. Each subject was paid according to the speed and accuracy of her classifications. Specially, the incentive scheme is: Payout $= \$(20 \times accuracy - 10 \times avgseconds)$, where "*accuracy*" is the percentage of trials where the subject correctly classified $X$ as larger or smaller than 65, and "*avgseconds*" is the average amount of time it took the subject to classify a number throughout the experiment, in seconds. Standard errors in parentheses are clustered at the subject level, and ***, **, * denote statistical significance at the 1%, 5%, and 10% levels, respectively.

| | (1) | (2) | (3) |
|---|---|---|---|
| Dependent variable: "Classify $X$ as greater than 65" | All data | $51 \leq X \leq 79$ | $X < 60$ or $X \geq 70$ |
| *high* | 0.00 | 0.04 | –0.07 |
| | (0.02) | (0.05) | (0.04) |
| $\ell$n$(X/65)$ | 19.53*** | 19.53*** | 17.45*** |
| | (2.09) | (2.09) | (1.58) |
| $\ell$n$(X/65) \times high$ | –9.71*** | –3.56*** | –7.98*** |
| | (1.11) | (0.95) | (0.69) |
| Constant | 0.20*** | 0.20*** | 0.30*** |
| | (0.07) | (0.07) | (0.08) |
| Pseudo $R$-squared | 0.53 | 0.48 | 0.63 |
| Observations | 16,640 | 11,892 | 12,807 |

# Appendices

## A. Theoretical Derivations

### 1. *Proof of Proposition 1*

For a given prior distribution $f(\theta)$, we construct a class of likelihood functions that satisfies the efficient coding condition in equation (6) of the main text. To do so, we follow Wei and Stocker (2015) by making the change of variable $\tilde{\theta} = F(\theta)$, where $F(\theta) = \int_{-\infty}^{\theta} f(\xi)d\xi$ is the cumulative density function of $\theta$. We think of $\tilde{\theta}$ as the stimulus value in a "sensory space."

We first show that the efficient coding condition is satisfied in this sensory space if the transformed likelihood function $f(m|\tilde{\theta})$ is *location-independent*:

$$f(m|\tilde{\theta}) = g(\tilde{\theta} - m), \tag{A.1}$$

where $g(\cdot)$ is some smooth density function that integrates to one.

To prove this statement, first note that equation (A.1) allows us to write the Fisher information in the sensory space as

$$\begin{aligned} J(\tilde{\theta}) &= \int_{-\infty}^{\infty} \left( \frac{\partial \ell \mathrm{n}\, f(m|\tilde{\theta})}{\partial \tilde{\theta}} \right)^2 f(m|\tilde{\theta}) dm \\ &= \int_{-\infty}^{\infty} \left(g'(\alpha)\right)^2 g^{-1}(\alpha) d\alpha = C, \end{aligned} \tag{A.2}$$

where $C$ is a positive constant, and $\tilde{\theta} - m$ is denoted as $\alpha$. Also note that $\tilde{\theta}$ is uniformly distributed between zero and one in the sensory space. Therefore,

$$\sqrt{J(\tilde{\theta})} = \sqrt{C} \propto f(\tilde{\theta}) = 1 \tag{A.3}$$

for any $\tilde{\theta} \in [0, 1]$. That is, the efficient coding condition (6) is satisfied in the sensory space.

Next, we show that the assumption (A.1) implies that the efficient coding condition is also satisfied in the original stimulus space. By (A.1), the likelihood function in the original stimulus space is

$$f(m|\theta) = g(F(\theta) - m). \tag{A.4}$$

The Fisher information is

$$\begin{aligned} J(\tilde{\theta}) &= \int_{-\infty}^{\infty} \left( \frac{\partial \ell \mathrm{n}\, f(m|\theta)}{\partial \tilde{\theta}} \right)^2 f(m|\theta) dm \\ &= \left( \int_{-\infty}^{\infty} \left(g'(\alpha)\right)^2 g^{-1}(\alpha) d\alpha \right) f^2(\theta) = C \cdot f^2(\theta). \end{aligned} \tag{A.5}$$

As a result,

$$\sqrt{J(\theta)} = \sqrt{C} \cdot f(\theta) \propto f(\theta) \tag{A.6}$$

for any $\theta \in (-\infty, \infty)$. That is, the efficient coding condition (6) is satisfied in the stimulus space.

In Proposition 1, we present the likelihood function $f(m|\theta)$ with a specific form for the function $g(\cdot)$ in (A.1): we assume $g(\cdot)$ is a normal density function with mean 0 and variance $\sigma^2$. This is in keeping with the requirement from Wei and Stocker (2016): when $g(\cdot)$ is normal and $\sigma$ is small, the condition in (6) is a good approximation for maximizing the mutual information in (2) of the main text subject to the capacity constraint in (3). Given this specific form of $g(\cdot)$, the likelihood function becomes

$$f(m|\theta) = \frac{1}{\sqrt{2\pi} \cdot \sigma} \exp\left(-\frac{(F(\theta) - m)^2}{2\sigma^2}\right). \tag{A.7}$$

This is the same as equation (7) in the main text. ■

### 2. *Properties of* $f(R_x)$

First, we show that the distribution of $R_x$ defined in equation (11) of the main text is independent of the shape of the stimulus distribution that the $DM$ expects. To prove this statement, we notice that the likelihood function $f(R_x|X)$ in (10) can be written as

$$f(R_x|X) = g(\int_0^X f(y; \mu_x, \sigma_x)dy - R_x), \tag{A.8}$$

where $g(\cdot)$ is a normal density function with mean zero and variance $\sigma^2$, and $f(y; \mu_x, \sigma_x)$ is from (8): it is the probability density function of a lognormal distribution. Equation (A.8) implies

$$\begin{aligned} f(R_x) &= \int_0^\infty f(R_x|X) f(X; \mu_x, \sigma_x)dX \\ = \int_0^\infty g(\int_0^X f(y; \mu_x, \sigma_x)dy - R_x) f(X; \mu_x, \sigma_x)dX &= \int_0^1 g(z - R_x)dz, \end{aligned} \tag{A.9}$$

where $z \equiv \int_0^X f(y; \mu_x, \sigma_x)dy$.

Equation (A.9) makes it clear that the distribution of $R_x$ does not depend on the shape of the stimulus distribution $f(X; \mu_x, \sigma_x)$: all continuous stimulus distributions lead to the same $f(R_x)$. Two assumptions together guarantee this "invariance" result. First, the likelihood function is location-independent in the sensory space (as we assume in equation (A.1)). Second, the transformation from the stimulus space to the sensory space is by the cumulative density function of the stimulus value.

**[Place Figure A1 about here]**

Next, we examine the asymptotic behavior of $f(R_x)$ as $\sigma$ goes to zero. From (A.9) we know that

$$f(R_x) = \int_0^1 g(z - R_x)dz \xrightarrow{\sigma \to 0} \int_0^1 \delta(z - R_x)dz = \begin{cases} 1 & 0 \leq R_x \leq 1 \\ 0 & \text{otherwise} \end{cases}, \tag{A.10}$$

where $\delta(\cdot)$ is a standard Dirac delta function. That is, in the limiting "noiseless" case, $f(R_x)$ converges to a uniform distribution between zero and one. To illustrate this point, Figure A1 plots $f(R_x)$ for $\sigma = 0.05$, 0.1, and 0.15. As $\sigma$ decreases, $f(R_x)$ indeed converges toward a uniform distribution. This result is a manifestation that, with vanishing noise, uniformity of $f(R_x)$ guarantees the optimality of the efficient coding condition in equation (6) of the main text. ■

## Figure A1. The distribution of the noisy signal $R_x$

The figure plots the unconditional distribution of the noisy signal, $f(R_x)$, according to equation (11) of the main text, for $\sigma = 0.05$, 0.1, and 0.15.

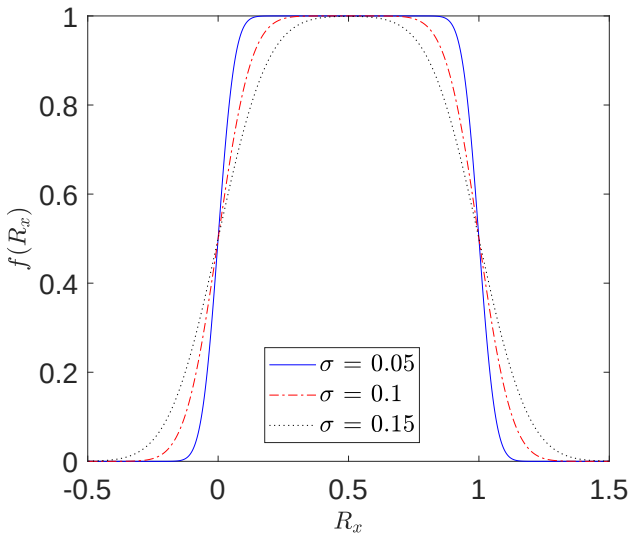

## B. Additional Analyses on Scale Invariance

In the discussion section of the main text, we noted that Weber's law does not hold universally in our model; it arises under a particular type of prior distribution—one in which there is a higher probability of smaller stimulus values, compared to larger stimulus values. In our choice environment, Weber's law would predict a type of "scale invariance," in which risk taking depends only on the ratio, $X/C$, but not on the separate levels of $X$ and $C$. This is a key prediction of the KLW model, and it stems, in part, from the logarithmic compression in the encoding function that is assumed for both $X$ and $C$. However, when the prior distribution is lognormal, our model of efficient coding does *not* imply logarithmic compression in the encoding functions.

To better understand how our model generates predictions that violate scale invariance, consider a choice set in which $X$ and $C$ are drawn from their respective lognormal distributions. Suppose further that, in this choice set, $C$ takes the mean value of its distribution, whereas $X$ is drawn from the left tail of its lognormal distribution. In this case, efficient coding implies that the $DM$ will be able to finely discriminate between $C$ and its nearby values, but she will not be able to discriminate well between $X$ and its nearby values. As a consequence, if we present the $DM$ with a new choice set by multiplying the original values of $X$ and $C$ by a common constant that is greater than one, then this multiplication will cause a substantial increase in the $DM$'s perceived valuation of $C$, but not of $X$. Therefore, the *perceived* ratio $X/C$ decreases on average, causing a reduction in risk taking, and hence, a violation of scale invariance.

A key ingredient of this argument, however, is that $X$ must be drawn from one of the tails of its distribution, so that the multiplier generates a smaller (percentage) increase in the perceived value of $X$, compared to that of $C$. If, instead, the values of $X$ and $C$ are both close to their respective mean values of the prior distributions, then a common multiplier should lead to a similar increase in the perception of each value, and therefore, only a small change in risk taking. Our model therefore predicts that large violations of scale invariance are not expected to occur often, since these violations occur only when one of the payoffs is drawn from the tails of its distribution.

**[Place Figure B2 about here]**

To assess this prediction quantitatively, we plot, in the upper panel of Figure B2, the model-implied probability of choosing the risky lottery as a function of $\ell\text{n}(X/C)$, for three different regions of $X$: $(i)$ low values of $X$ (bottom 30% of its distribution); $(ii)$ intermediate values of $X$ (between $30^{th}$ and $70^{th}$ percentile of its distribution); and $(iii)$ high values of $X$ (top 30% of its distribution). Each point in the figure represents a single choice set and its model-implied probability of choosing the risky lottery. The values of $X$ and $C$ are generated over equally spaced grid points of $[X_{min}, X_{max}] \times [C_{min}, C_{max}] = [4, 50] \times [2.5, 25]$.

The figure clearly shows violations of scale invariance: for a given value of $\ell\text{n}(X/C)$, the model-implied probability depends on whether $X$ is drawn from the left tail (in blue), the intermediate

region (in red), or the right tail (in black). As expected, these violations are most severe for choice sets in which $X$ is drawn from the left tail, and specifically, when $\ell n(X/C)$ is relatively large. In order for $X$ to be drawn from the left tail and for $\ell n(X/C)$ to be relatively large, $C$ must *also* be drawn from its left tail, which makes the occurrence of these particular choice sets very rare. Thus, the largest violations of scale invariance occur for those choice sets that are rarely presented to the $DM$. In contrast, the points in red, which represent the most likely values of $X$, fall roughly on the same curve, consistent with the model predicting an approximate scale invariance among these likely values of $\ell n(X/C)$.

To assess whether our experimental data are consistent with scale invariance, we also cut the data into the three subsamples of $X$ described above. For each of the subsamples, we plot, in the bottom panel of Figure B2, the risky choice data using 20 bins, where each bin contains an equal number of trials; this binning procedure is important because it controls for the frequency that each value of $\ell n(X/C)$ is presented in our experiment. The data are noisy since we cut them into three subsamples and analyze only the high volatility condition. However, an important feature to note is that, for each value of $\ell n(X/C)$ in the figure—which is weighted by its frequency of being presented in the experiment—the probability of risk taking varies only slightly with the level of $X$.

In summary, our model predicts that risk taking will depend on the level of $X$ and $C$. Moreover, our model predicts that this dependence is concentrated mainly among outlier values, for which the $DM$ has difficulty discriminating between nearby values. Among payoffs that the $DM$ is most likely to observe in a choice set, our model predicts that risk taking should be approximately scale invariant. We find that this prediction is broadly consistent with our experimental data.

## Figure B1. Probability of risk taking as a function of $X$ and $C$

The figure plots the probability of risk taking computed in equation (18) of the main text, for two different volatility levels of the stimulus distribution, $\sigma_x = \sigma_c = 0.19$ (low volatility) and $\sigma_x = \sigma_c = 0.55$ (high volatility). The parameter values are: $\mu_x = 3.05$, $\mu_c = 2.35$, $p = 0.59$, and $\sigma = 0.1$.

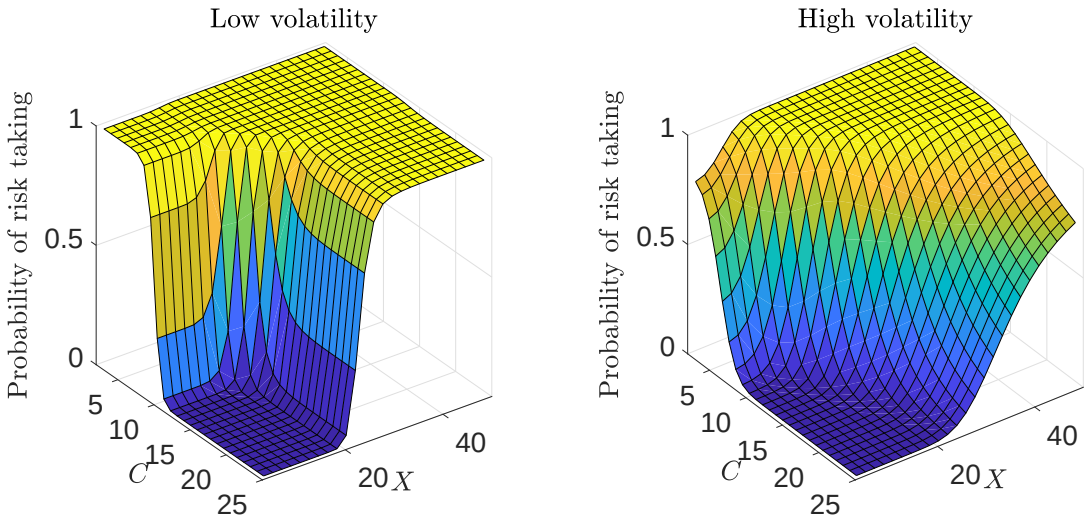

## Figure B2. Probability of risk taking for different levels of $X$

The upper panel plots the model-implied probability of risk taking in the high volatility condition ($\sigma_x = \sigma_c = 0.55$), for three different intervals of $X$: (*i*) *Blue*: low values of $X$ (bottom 30% of distribution); (*ii*) *Red*: intermediate values of $X$ (between $30^{th}$ and $70^{th}$ percentile of distribution); and (*iii*) *Black*: high values of $X$ (top 30% of distribution). Each point in the figure represents a single choice set and its model-implied probability of choosing the risky lottery. The bottom panel plots the experimental data from the (same) high volatility condition. For each of the three different intervals of $X$, we place the values of $\ell\text{n}(X/C)$ into 20 equally sized bins. For each bin, we then compute the average value of $\ell\text{n}(X/C)$ and the associated average level of risk taking. For the upper panel, we set $\sigma = 0.1$.

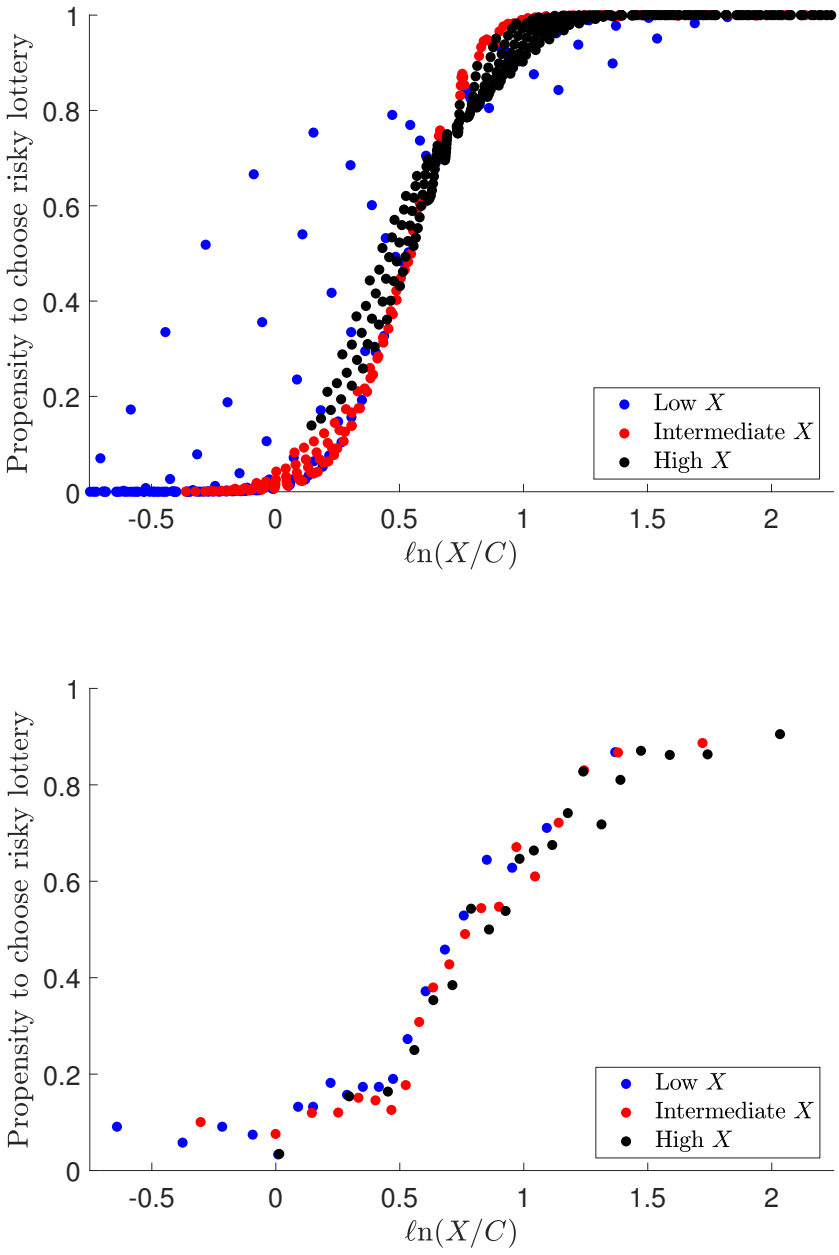

# C. Experiment Three: A Test Between Alternative Definitions of Efficiency

Section VI.1 of the main text discussed different definitions of efficient coding. Here we report further details on the third experiment we conducted to test an alternative definition of efficiency.

## 1. *Design*

The design of our third experiment is almost identical to the perceptual experiment described in Section IV. The only change we make is to the incentive scheme. In particular, we still pay subjects according to the payout equation, $\$(20 \times accuracy - 10 \times avgseconds)$, but importantly we only compute *accuracy* and *avgseconds* on trials in which $X$ lies in the range $[51, 79]$. This incentive scheme implies that subjects are paid on all trials in the low volatility condition, but only on a subset of trials in the high volatility condition. Compared to our original perceptual experiment, all other design features remain the same. The experimental instructions for this task can be found in Appendix E.

## 2. *Experimental procedures*

The experimental procedures for this task are almost identical to those that we reported in Section IV. The main difference, apart from the incentive scheme, is that we recruited $N = 16$ subjects from USC for this experiment. The average earning, including a \$7 show-up fee, was \$20.04.

## 3. *Experimental results*

Overall, subjects accurately classified the stimuli on 93.3% of trials with an average response time of 0.53 seconds. On those trials in which subjects were incentivized, accuracy was 92.2% and the average response time was 0.54 seconds.

**[Place Figure C1 about here]**

Figure C1 shows the proportion of trials that subjects classified the stimulus as greater than 65, for each value of $X$. In the payoff-relevant range of $[51, 79]$, we find that subjects correctly classified stimuli on 90.6% of trials in the high volatility condition, and on 92.9% of trials in the low volatility condition. Thus, we replicate the results from our original perceptual experiment whereby subjects are significantly more accurate—in the range $[51, 79]$—in the low volatility condition compared to the high volatility condition ($p$-value $= 0.004$).

**[Place Table C1 about here]**

We also conduct tests for a difference in slope across our two experimental conditions, and report the results in Table C1. Column (1) shows that, consistent with the definition of efficiency that maximizes mutual information, the slope is steeper in the low volatility condition compared to the high volatility condition. Column (2) re-estimates the regression using data only in the payoff-relevant range $51 \leq X \leq 79$. We find that, in this subset of the data, the sensitivity to stimuli continues to be stronger in the low volatility condition. This finding lends further support to our model assumption that some coding resources are allocated toward stimulus values that are not directly payoff-relevant.

## Figure C1. Classification performance in Experiment Three

The $x$-axis denotes the integer $X$ that is presented on each trial. The $y$-axis denotes the proportion of trials for which subjects classified the integer $X$ as greater than 65. Data are pooled across trials and subjects, but are disaggregated by the high and low volatility conditions. In the high volatility condition, the integers are drawn uniformly from $[31, 99]$. In the low volatility condition, the integers are drawn uniformly from $[51, 79]$. Each subject was paid according to the accuracy and speed of her classifications. Specifically, the incentive scheme is: Payout $= \$(20 \times accuracy - 10 \times avgseconds)$, where "*accuracy*" is the percentage of trials where the subject correctly classified $X$ as larger or smaller than 65, and "*avgseconds*" is the average amount of time it took the subject to classify a number throughout the experiment, in seconds. Importantly, accuracy and speed are computed based on a subset of trials in which $X$ is in the range $[51, 79]$.

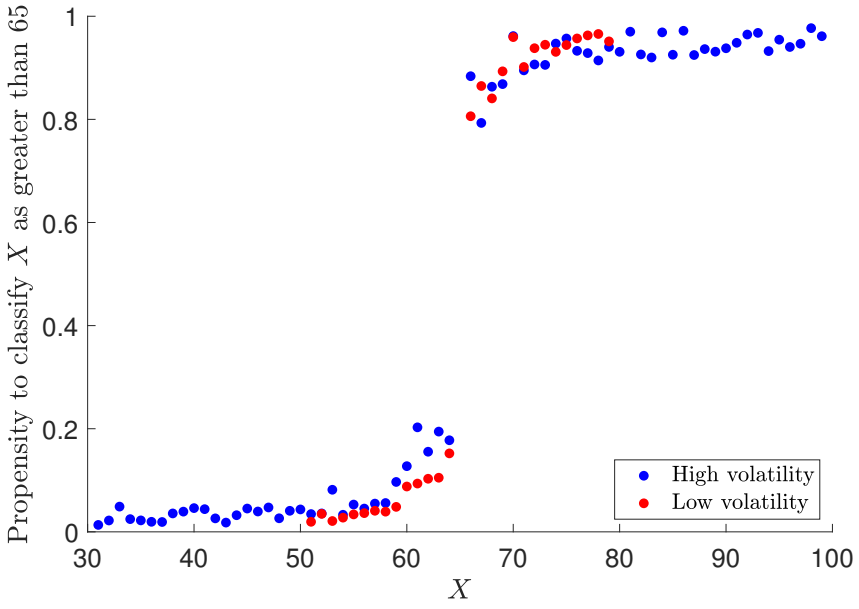

## Table C1. Probability of classification in Experiment Three

The table reports results from logistic regressions where the dependent variable takes the value of one if the subject classified the stimulus, $X$, as larger than 65, and zero otherwise. The dummy variable *high* takes the value of one if the trial belongs to the high volatility condition, and zero if it belongs to the low volatility condition. In the high volatility condition, the integer $X$ is drawn uniformly from $[31, 99]$, while in the low volatility condition, the integer is drawn uniformly from $[51, 79]$. Each subject was paid according to the accuracy and speed of her classifications. Specifically, the incentive scheme is: Payout $= \$(20 \times accuracy - 10 \times avgseconds)$, where "*accuracy*" is the percentage of trials where the subject correctly classified $X$ as larger or smaller than 65, and "*avgseconds*" is the average amount of time it took the subject to classify a number throughout the experiment, in seconds. Importantly, accuracy and speed are computed based on the subset of trials in which $X$ is in the range $[51, 79]$. Standard errors in parentheses are clustered at the subject level, and ***, **, * denote statistical significance at the 1%, 5%, and 10% levels, respectively.

| | (1) | (2) | (3) |
|---|---|---|---|
| Dependent variable: "Classify $X$ as greater than 65" | All data | $51 \leq X \leq 79$ | $X < 60$ or $X \geq 70$ |
| *high* | 0.13* | 0.13* | 0.05 |
| | (0.07) | (0.07) | (0.06) |
| $\ell$n$(X/65)$ | 25.43*** | 25.43*** | 21.56*** |
| | (4.37) | (4.37) | (3.02) |
| $\ell$n$(X/65) \times high$ | –14.48*** | –5.11** | –11.17*** |
| | (2.83) | (2.20) | (1.68) |
| Constant | –0.06 | –0.06 | 0.08 |
| | (0.05) | (0.05) | (0.10) |
| Pseudo $R$-squared | 0.61 | 0.58 | 0.70 |
| Observations | 20,480 | 14,477 | 15,807 |

## D. Comparing the Predictions of Efficient Coding and Salience Theory for the Risky Choice Experiment

Here we provide a comparison of our model with salience theory of choice under risk (Bordalo et al. (2012)) (henceforth BGS). Under salience theory, attention is drawn toward salient payoffs, which are then overweighted relative to their objective probabilities. According to BGS, "a lottery payoff is salient if it is very different in percentage terms from the payoffs of other available lotteries" (pg. 1244). This definition captures two important psychological properties: $(i)$ perception is based on the difference between stimuli; and $(ii)$ it becomes more difficult to detect a given difference between two stimuli as the *level* of each stimulus increases.

While both efficient coding and salience theory provide models of distorted perception in risky choice, the mechanisms that generate this distortion are distinct. In our experiment, there are two potential sources of uncertainty: $(i)$ the $DM$ has imperfect perception and is therefore uncertain about the payoff values that characterize each lottery—$X$ and $C$ in our experiment—even after the choice set is presented; and $(ii)$ the $DM$ is exposed to the more standard source of uncertainty whereby, if she chooses the risky lottery, she is uncertain about whether she will receive $X$ (with probability $p$) or zero (with probability $1-p$). In our model of efficient coding, only the first source of uncertainty triggers the mechanism that distorts perception. Conditional on the distorted perception of the payoff values, the $DM$ then handles the second source of risk in the standard way by selecting the lottery with the highest expected value.

In contrast, salience theory assumes that only the second source of uncertainty—regarding the outcome of the risky lottery $(X, p; 0, 1-p)$—is relevant. There is no uncertainty about the payoff values that characterize each lottery; the $DM$ observes $X$ and $C$ perfectly. Instead, these payoffs differentially attract the $DM$'s attention, which distorts the decision weight associated with each payoff.

It is worth noting that, even though salience theory assumes that payoffs are perceived without noise, the theory can easily be applied to the case in which the $DM$'s only source of uncertainty is about the payoff values that are presented in the choice set. In this case, we can think of there being a continuum of states, and each state delivers a pair $(X, C)$. In this framework, the $DM$'s choice would then be between the two *priors* that generate $X$ and $C$. Notice that this decision is not the one that subjects in our experiments face. Nonetheless, salience theory makes sharp predictions about which payoffs are overweighted. In particular, we show below that the $DM$ overweights outlier values of $X$, which in turn distorts the perceived valuation of each prior.

After analyzing the effect of salience when the $DM$'s only source of uncertainty is about the payoff values in the choice set, we then examine the second source of uncertainty. Here, we assume that the $DM$ has perfect information about the payoff values in the choice set, but now faces uncertainty about which outcome the risky lottery will deliver. This second application of salience

theory is more closely aligned with our experimental setup, and we find that the theory does a good job explaining the basic features of our data.

### 1. *Salience model*

Salience theory operates by distorting the weight on each state payoff for a given lottery. Here we consider the case in which the choice set contains only two lotteries, $L^1$ and $L^2$. We define a state space $S$, where each $s \in S$ occurs with probability $p_s$, and lottery $L^i$ delivers payoff $x_s^i$ in state $s$. As in our model of efficient coding, we assume the $DM$ uses a linear value function $v(z) = z$. Without any salience distortions, the value of lottery $L^i$ is given by:

$$V(L^i) = \sum\nolimits_{s \in S} p_s \cdot x_s^i. \tag{D.1}$$

The salience model departs from this valuation equation by assuming that the $DM$ does not use the set of objective probabilities $\{p_s;\ s \in S\}$, but instead uses a set of decision weights for lottery $L^i$ denoted by $\{\pi_s^i; s \in S\}$, where $\pi_s^i = p_s \omega_s^i$ for each state $s$. The distortion factor $\omega_s^i$ distorts the objective probability, and is defined as:

$$\omega_s^i = \frac{\delta^{-\sigma(x_s^i, x_s^{-i})}}{\sum_{r \in S} \delta^{-\sigma(x_r^i, x_r^{-i})} \cdot p_r}. \tag{D.2}$$

In the above equation, $\delta \in (0, 1]$ captures the degree to which salience distorts objective probabilities. $\sigma(x_s^i, x_s^{-i})$ is the *salience function* which maps state payoffs delivered by $L^i$ and $L^{-i}$ into a salience measure. This function formalizes features of human perception; for our experimental setup, the two most important properties of the salience function are ordering and diminishing sensitivity. Ordering implies that states in which there is a larger difference between payoffs (across lotteries) are more salient. This captures the intuition that attention is drawn toward attributes with larger differences. Diminishing sensitivity implies that adding a constant to all payoffs in a state will decrease the salience of that state.[24] As discussed in Section VI.4, diminishing sensitivity is an exogenous assumption in salience theory, but it arises endogenously in our model of efficient coding.

We use a particular functional form of the salience function that satisfies ordering and diminishing sensitivity:

$$\sigma(x_s^i, x_s^{-i}) = \frac{|x_s^i - x_s^{-i}|}{|x_s^i| + |x_s^{-i}| + \theta}, \tag{D.3}$$

where $\theta > 0$ controls the degree of diminishing sensitivity. Given this salience function, the valuation

[24] As BGS put it, "the intensity with which payoffs in a state are perceived increases as the state's payoffs approach the status quo of zero..." (pg. 1254).

of lottery $L^i$ under salience theory is given by:

$$V(L^i) = \sum\nolimits_{s \in S} \pi_s \cdot x_s^i. \tag{D.4}$$

It follows that a payoff is overweighted, relative to its objective probability, $p_s$, if and only if $\omega_s^i > 1$. The $DM$ then chooses lottery $L^1$ if and only if $V(L^1) > V(L^2)$.

### 2. *Case 1: Applying salience theory when the DM is only uncertain about payoff values*

Recall that there are two potential sources of uncertainty that the $DM$ faces in our experiment. First, the $DM$ can be uncertain about the payoff values $(X, C)$ that characterize the risky lottery and the certain option in the choice set. Second, conditional on knowing these values of $X$ and $C$, the $DM$ can be uncertain about which outcome will obtain from the risky lottery: $X$ (with probability $p$) or zero (with probability $1-p$). In this section, we apply salience theory to the first source of uncertainty, in which the $DM$ is uncertain only about the values of $X$ and $C$. We can then think of $L^1$ as delivering a random payoff $X$ and $L^2$ as delivering a random payoff $C$. As in our experiment, we assume that the values of $X$ and $C$ are jointly drawn from a lognormal distribution:

$$\begin{pmatrix} \ell\mathrm{n}X \\ \ell\mathrm{n}C \end{pmatrix} \sim \mathcal{N}\left( \begin{pmatrix} \mu_x \\ \mu_c \end{pmatrix}, \begin{pmatrix} \sigma_x^2 & \rho\sigma_x\sigma_c \\ \rho\sigma_x\sigma_c & \sigma_c^2 \end{pmatrix} \right). \tag{D.5}$$

As a result, in state $s$ in which $L^1$ delivers $X_s$, $L^2$ will on average deliver[25]

$$\mathbb{E}[\tilde{C}|X_s] = \exp\left( \mu_c + \frac{\rho\sigma_c}{\sigma_x}(\ell\mathrm{n}X_s - \mu_x) + \frac{1}{2}\sigma_c^2(1-\rho^2) \right). \tag{D.6}$$

The salience measure for $L^1$ in state $s$ is then given by:

$$\sigma(X_s, \mathbb{E}[\tilde{C}|X_s]) = \frac{\left| X_s - \exp\left( \mu_c + \frac{\rho\sigma_c}{\sigma_x}(\ell\mathrm{n}X_s - \mu_x) + \frac{1}{2}\sigma_c^2(1-\rho^2) \right) \right|}{X_s + \exp\left( \mu_c + \frac{\rho\sigma_c}{\sigma_x}(\ell\mathrm{n}X_s - \mu_x) + \frac{1}{2}\sigma_c^2(1-\rho^2) \right) + \theta}. \tag{D.7}$$

For each $X_s$, we can then compute its distortion factor for $L^1$ as

$$\omega^1(X_s) = \frac{\delta^{-\sigma(X_s, \mathbb{E}[\tilde{C}|X_s])}}{\int_0^\infty f(X; \mu_x, \sigma_x)\delta^{-\sigma(X, \mathbb{E}[\tilde{C}|X])}dX}, \tag{D.8}$$

where $f(X; \mu_x, \sigma_x) = \frac{1}{X\sigma_x\sqrt{2\pi}} \exp\left( -\frac{(\ell\mathrm{n}X - \mu_x)^2}{2\sigma_x^2} \right)$ is a lognormal probability density function.

[25] To justify comparing $X$ with the average realization of $C$ when computing the salience function for $X$, one can think that for each value of $X$, there is a continuum of other assets with different realized payoffs of $C$.

Below we plot $\omega^1(X)$ as a function of $X$, for the parameter values we used in our risky choice experiment: $\mu_x = 3.05$, $\mu_c = 2.35$, $\sigma_x = \sigma_c = 0.55$, and $\rho = 0.5$. For salience-based parameters, we set $\delta = 0.7$ and $\theta = 0.1$, consistent with the point estimates in BGS.

**[Place Figure D1 about here]**

We see that very large values of $X$ draw the $DM$'s attention, and these payoffs are overweighted (their distortion factors are greater than one). To be clear, large values of $X$ are not salient because they themselves are large. Rather, large values of $X$ are salient, because when they are compared to the average payoff of $L^2$, $\mathbb{E}[\tilde{C}|X]$, the *difference* is large. By the same logic, very small values of $X$ are also salient, and thus overweighted.[26]

Without any salience distortions, it is clear that the $DM$ would always prefer $L^1$ over $L^2$ because the lotteries are the same except $L^1$ has a strictly higher mean. Indeed, for $\delta = 1$, $V(L^1) - V(L^2) = 12.37$. However, for $\delta = 0.7$ and $\theta = 0.1$, we find that $V(L^1) - V(L^2) = 13.22 > 12.37$. That is, lottery $L^1$ becomes relatively more attractive because its extreme payoffs are overweighted. This prediction is thus consistent with the intuition that outlier payoffs are overweighted, and hence drive choice in favor of the lottery $L^1$.

We emphasize that with our experimental data, we cannot test the above prediction. In our risky choice experiment, subjects are *not* given the choice between the two "prior" lotteries. Rather, they are given the choice between two lotteries that are characterized by *draws* from these two priors. In the next section, we examine the predictions of salience theory, conditional on these realized draws.

### *3. Case 2: Applying salience theory when the DM is certain about payoff values*

Now consider the more standard case in which the $DM$ has no uncertainty about the payoff values in the choice set. In this case, the only source of uncertainty is about the outcome of the risky lottery, $(X, p; 0, 1-p)$. There are two possible states of the world: $s \in \{up, down\}$. In the *up* state (with probability $p$), the risky lottery delivers a payoff of $X$; and in the *down* state (with probability $1-p$), the risky lottery delivers a payoff of zero. In both states, the certain option delivers a payoff of $C$.

To examine the basic explanatory power of the salience model, we set $\delta = 0.7$ and $\theta = 0.1$, and plot the probability of choosing the risky lottery against $V(\text{risky lottery}) - V(\text{certain option})$. Figure D2 shows that the probability of choosing the risky lottery increases in the difference between the two subjective lottery values.[27] This is, however, not a particularly strong test of salience theory:

[26] For the parameter values used in Figure D1, the ordering feature of the salience function $\sigma(\cdot,\cdot)$ dominates diminishing sensitivity as $X$ and $\mathbb{E}[\tilde{C}|X]$ get larger. However, if we set $\mu_c = 3.55 > \mu_x = 3.05$, and set $\rho = 0.9$, then diminishing sensitivity dominates ordering. That is, $\omega^1$ would *decrease* in $X$ as $X$ becomes very large.

[27] This prediction is robust to different values of $\delta$ in $(0, 1]$.

by and large, the observed variation in choice behavior across trials is driven by variation in payoff values, without much variation in their salience.[28]

**[Place Figure D2 about here]**

A more noteworthy feature of Figure D2 is that the slope of the probability of risk taking curve is greater for the low volatility condition compared to the high volatility condition; this result resembles Figure 5 in the main text. In the basic version of the salience model outlined above, risk taking is independent of whether the choice set is presented in the low volatility or high volatility condition. This invariance result is driven by the assumption that only payoffs in the current choice set affect perception. Efficient coding, on the other hand, predicts that perception depends systematically on the payoff distribution to which the subject has recently adapted. In particular, efficient coding allows the degree of diminishing sensitivity to fluctuate based on past payoffs, which helps generate the different slopes observed in Figure D2. For salience theory to account for this slope difference, one could generalize the salience function in equation (D.3) by allowing past payoffs to affect the salience of current payoffs. In this way, salience theory would generate context dependence in both the time series and the cross-section. Some guidance for this approach of using past experiences to form a perception of the current choice set is given in Bordalo et al. (2019), although applications in that model focus mainly on riskless choice.

### *4. Summary*

A key intuiton from salience theory is that outlier values are salient, and therefore attract the $DM$'s attention and increase the decision weights associated with these values. Indeed, when analyzing the first source of uncertainty about the payoff values of $X$ and $C$ that characterize the choice set, we showed that extreme values of $X$—both very small and very large values—are overweighted. However, these implications apply to an environment in which the $DM$ chooses between the two lognormal priors. These are not the lotteries presented to subjects in our risky choice experiment.

Instead, our experiment presents subjects with lotteries $\{(X, p; 0, 1-p), (C, 1)\}$, in which $X$ and $C$ are the realized values from the two lognormal priors. In this case, there are only two states, *up* and *down*. When applying salience theory to this simple choice problem, the theory does a good job explaining the data, except for the difference in slopes across the two volatility conditions (Figure D2).

[28] For $\theta = 0.1$, the *down* state is salient for *all* choice sets in our experiment. This result is robust to different values of $\theta$. For example, if we reduce the degree of diminishing sensitivity by setting $\theta = 10$, then the *down* state remains salient in 93% of the trials.

**Figure D1. Distortion factor $\omega^1$ for lottery $L^1$ as a function of payoff $X$**

We plot the distortion factor $\omega^1(X)$ from equation (D.8) as a function of $X$. The parameter values are: $\mu_x = 3.05$, $\mu_c = 2.35$, $\sigma_x = \sigma_c = 0.55$, $\rho = 0.5$, $\delta = 0.7$, and $\theta = 0.1$.

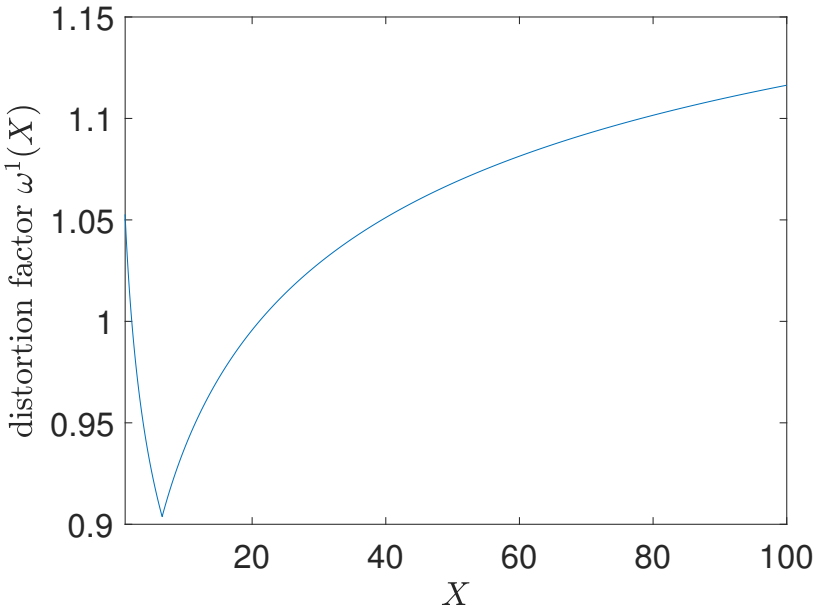

**Figure D2. Probability of risk taking as a function of salience implied lottery valuations**

We first compute the valuations of the risky lottery and certain option, $V(\text{risky lottery})$ and $V(\text{certain option})$, both under salience theory. We use the salience function in equation (D.3) and the distortion factor in equation (D.2), with $\delta = 0.7$, $\theta = 0.1$, and $s \in \{up, down\}$. We then plot the proportion of trials on which subjects choose the risky lottery as a function of $V(\text{risky lottery}) - V(\text{certain option})$, for both the high volatility condition ($\sigma_x = \sigma_c = 0.55$) and the low volatility condition ($\sigma_x = \sigma_c = 0.19$). Data are pooled across trials and subjects. For each of the two volatility conditions, we bin the $V(\text{risky lottery}) - V(\text{certain option})$ variable into two-hundred bins such that each bin has an equal number of trials. The figure is analogous to Figure 5 in the main text.

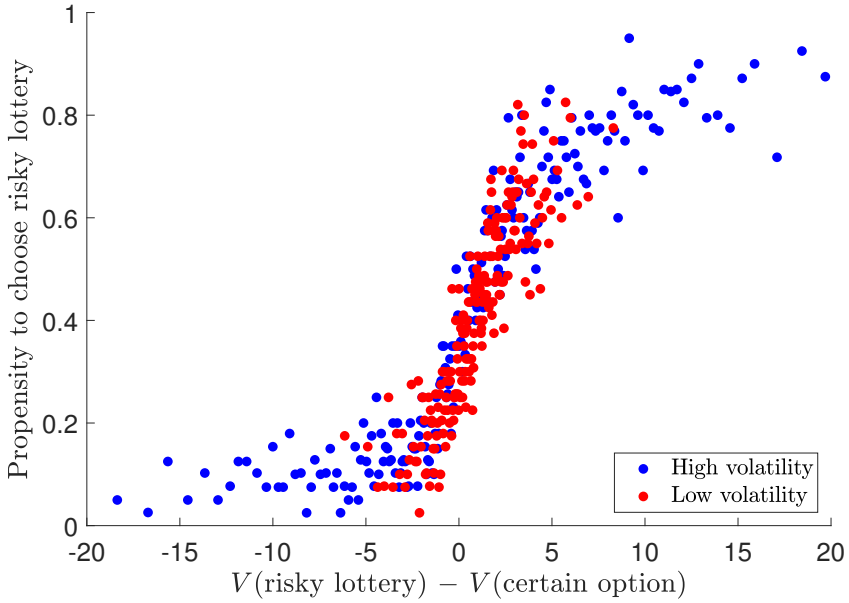

# E. Experimental Instructions

## 1. *Instructions for the main risky choice task*

Experiment Instructions

Thank you for participating in this experiment. Before we begin, please turn off all cell phones and put all belongings away. For your participation, you have already earned $7, and you will have the opportunity to earn more money depending on your answers during the experiment.

In the experiment, you will be asked to make a series of decisions about choosing a "risky gamble" or a "sure thing". The risky gamble will pay a positive amount with 59% chance, and $0 with 41% chance. The amount shown for the sure thing will be paid with 100% chance, if chosen. Below is an example screen from the experiment:

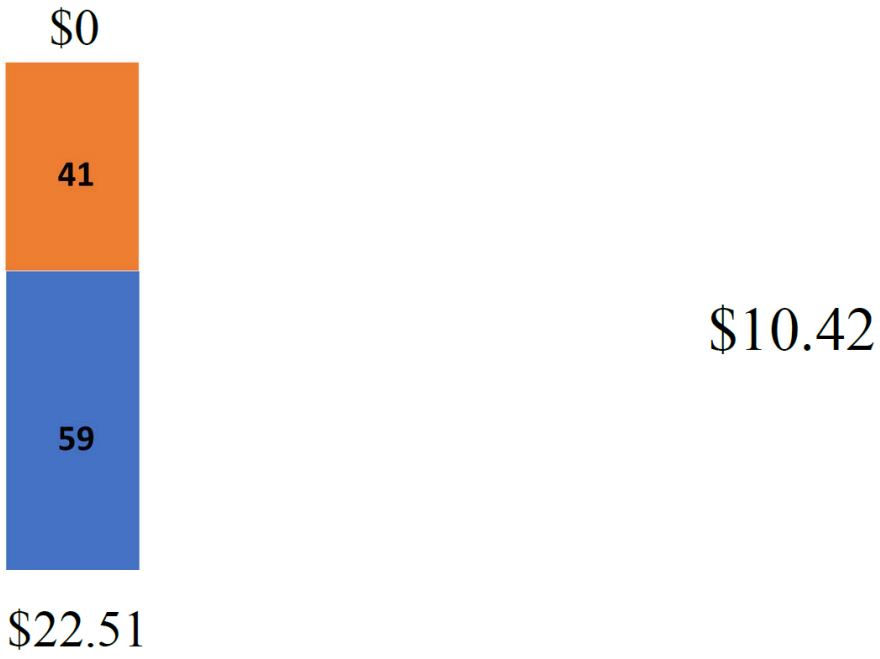


In this example, the risky gamble pays $22.51 with 59% chance, and $0 with 41% chance. The sure thing pays $10.42 with 100% chance. You will be asked to select one of the two options for each question in the experiment. The experiment is broken down into eight parts, and each part contains sixty questions.

At the end of the experiment, one trial will be randomly selected, and you'll be paid according to your decision on that trial. For example, if the above trial was chosen, and you selected the sure thing you would be paid a total of $10.42 + $7 = $17.42. If instead you chose the risky gamble, you'd be paid either $7 or ($22.51 + $7) = $29.51, depending on which outcome the computer randomly selects. Before we begin, you will see 10 practice trials to familiarize yourself with the software. These 10 practice trials will not count toward the real experiment.

*2. Instructions for the perceptual task*

Experiment Instructions

Thank you for participating in this experiment. Before we begin, please turn off all cell phones and put away all belongings until the end of the experiment. For your participation, you have already earned $7, and you will have the opportunity to earn more money depending on your answers during the experiment.

In the experiment, you will see a series of numbers and will be asked to classify whether the number is larger or smaller than the number "65". If the number is larger than 65, press the "?" key, and if it is smaller than 65, press the "z" key. At the end of the experiment, you will be paid depending on the speed and accuracy of your classifications. Specifically, you will be paid:

$$\text{Payout} = \$(20 \times accuracy - 10 \times avgseconds),$$

where "*accuracy*" is the percentage of trials where you correctly classified the number as larger or smaller than 65. "*avgseconds*" is the average amount of time it takes you to classify a number throughout the experiment, in seconds. For example, if you correctly classified all trials and it took you 0.3 seconds to respond to each question, you would earn $\$(20 \times 100\% - 10 \times 0.3) = \$17.00$ (plus the $7 show-up fee). If instead you only answer 75% of the questions accurately and took 1 second to respond to each question, you would be paid $\$(20 \times 75\% - 10 \times 1) = \$5.00$ (plus the $7 show-up fee). Therefore, you will make the most money by answering as quickly and as accurately as possible.

The experiment will be separated into sixteen parts, and each part will contain 80 trials. In between each part, you can take a short (~1 minute) break, and then continue at your own pace. When you finish all sixteen parts, please raise your hand and do not disturb other subjects.

Before you begin the experiment, you will go through 10 practice trials to familiarize yourself with the software. These 10 practice trials will not be counted when computing your final payout.

*3. Instructions for the perceptual task with restricted payout*

Experiment Instructions

Thank you for participating in this experiment. Before we begin, please turn off all cell phones and put away all belongings until the end of the experiment. For your participation, you have already earned $7, and you will have the opportunity to earn more money depending on your answers during the experiment.

In the experiment, you will see a series of numbers and will be asked to classify whether the number is larger or smaller than the number "65". If the number is larger than 65, press the "?" key, and if it is smaller than 65, press the "z" key. At the end of the experiment, you will be paid depending on the speed and accuracy of your classifications. Specifically, you will be paid:

$$\text{Payout} = \$(20 \times \textit{accuracy} - 10 \times \textit{avgseconds}),$$

where "*accuracy*" is the percentage of trials where you correctly classified the number as larger or smaller than 65. "*avgseconds"* is the average amount of time it takes you to classify a number throughout the experiment, in seconds. Importantly, we will compute your measure of accuracy and speed based only on a subset of trials. Specifically, we will only compute your accuracy and speed based on those trials where the number is in the range [51, 79]. For instance, if the number "78" is shown on a given trial, your classification will count toward your accuracy and speed measurement. If instead the number shown is "80", your classification on this trial will not count toward your accuracy or speed measurement.

Suppose you correctly classified the number on all trials and it took you 0.3 seconds to respond to each question, you would earn $\$(20 \times 100\% - 10 \times 0.3) = \$17.00$ (plus the $7 show-up fee). If instead you only correctly classified the number on 60% of trials and it took you 1 second to respond to each question, you would be paid $\$(20 \times 60\% - 10 \times 1.0) = \$2.00$ (plus the $7 show-up fee). Therefore, you will make the most money by classifying as quickly and accurately as possible, on those trials where the number is in the range [51, 79].

The experiment will be separated into sixteen parts, and each part will contain 80 trials. In between each part, you can take a short break, and then continue at your own pace. When you finish all sixteen parts, please raise your hand and do not disturb other subjects.

Before you begin the experiment, you will go through 10 practice trials to familiarize yourself with the software. These 10 practice trials will not be counted when computing your final payout.